Design and Development of an I-V Curve Tracing and Electrical Performance Analyzing System for Solar Photovoltaic Module

A thesis Presented to the Institute of Energy at University of Dhaka, Bangladesh in partial fulfillment of the requirements for the degree of Masters of Science in Renewable Energy and Technology

Submitted by

Md. Abu Sayed Siddique Masud
Exam Roll: 421
Registration No: Ha- 323
Session: 2013-2014
&
Mahiuddin Mahmud Romel
Exam Roll: 414
Registration No: Ha- 304
Session: 2013-2014

Supervised By

Dr. Md. Habibur Rahman
Professor
Department of Electrical and Electronic Engineering
University of Dhaka
Dhaka, Bangladesh

February, 2016

DECLARATION

This is to certify that we have done this work and to the best of our knowledge it contains no materials which are exactly same which were previously published anywhere in print/soft media or has not been submitted for any degree. Materials of work founded by other researchers are mentioned by reference.

Authors

_____
Md. Abu Sayed Siddique Masud

_____
Mahiuddin Mahmud Romel

CERTIFICATE

This is to certify that the project work entitled "Design and Development of an I-V Curve Tracing and Electrical Performance Analyzing System for Solar Photovoltaic Module" by Md. Abu Sayed Siddique Masud (Registration No. Ha-323) and Mahiuddin Mahmud Romel (Registration No. Ha-304) has been carried out under my supervision, meets acceptable standard and can be submitted for evaluation to the Institute of Energy in partial fulfillment of the requirements for the degree of Masters of Science (MS) in Renewable Energy Technology.

Thesis Supervisor

_____

Dr. Md. Habibur Rahman
Professor
Department of Electrical and Electronic Engineering
University of Dhaka
Dhaka, Bangladesh
February, 2016

ACKNOLEDGEMENT

First of all, we are grateful to the Almighty to allow us to complete this project successfully in time.

We were extremely fortunate to work with Professor Dr. Md. Habibur Rahman, Department of Electrical and Electronic Engineering, University of Dhaka, who has given us continuous encouragement, valuable guidance and advice in all aspects related to this project.

We would like to express our thanks to Professor Dr. Saiful Huque, Director, Institute of Energy, University of Dhaka, for providing us the environment for the project continuation and never ending help throughout the time.

We extend our sincere thanks to Mr. Swapon Kumar Chowdhury for giving his valuable time whenever we needed and helped us throughout this project with the best of his knowledge.

We are also grateful to a lot of people for being so helpful and nice to us; some of the names we must keep in mind are Md. Mominul Islam for allowing us to use his lab, Saiful Islam for helping us with testing, Syed Asif Mahmood and Md. Mahmud Alam for helping us with the analyzing software tool.

It is nearly impossible to mention every name of the persons who have contributions any way in our work. We would like to thank for their encouragement and criticism which helped this work to be more enriched.

DEDICATION

To Our Parents

And

Teachers

Abstract

The electrical performance of a photovoltaic solar cell is described by its current–voltage (I–V) characteristic curve, which is in turn determined by device and material properties. This work presents a system capable of tracing current-voltage (I-V) characteristic curve and analyzing electrical performance characteristics of solar photovoltaic cells as well as modules. This system is divided into two main parts; firstly the current-voltage (I-V) data with temperature of the module at that instant, when it has brought under direct or diffused sun light, has been collected form the solar photovoltaic cell or module by means of some basic electronic circuits like current and voltage sensing using simple pulsed width modulation (PWM), MOSFET switching arrangement, liquid crystal display(LCD), keypad made with three selecting switch, temperature sensor, USB serial converter etc. These data has been stored in an EEPROM. Total system has a microcontroller to complete all the tasks it is programed for. Secondly the collected data transferred through an USB to TTL transfer system to the computer where it's going to be analyzed. To analyze the data collected from the module a handy analyzer software tool has been made in Java platform with Java programming language. Where we plot graphs of I-V and P-V characteristics curve and compare the results with the given module data. Thus long-term measurements of solar PV modules electrical performances in different operating modes and in different environments become possible through this system.

Table of Contents

List of Figures

List of Tables

List of Abbreviations

PV – Photovoltaic

EEPROM- Electrically Erasable Programmable Read-Only Memory

PWM- Pulsed Width Modulation

USB- Universal Serial Bus

μA- Micro Ampere

Ω- Ohm

mV- Millivolt

°C- Degree Celsius

I-V- Current-Voltage

MPP - Maximum Power Point

V_{MP}- Maximum Power Voltage

I_{MP}- Maximum Power Current

Voc- Open Circuit Voltage

Isc- Short Circuit Current

FF- Fill Factor

η- Efficiency

T- Temperature

MC- Microcontroller

MOSFET- Metal–Oxide–Semiconductor Field-Effect Transistor

LCD- Liquid Crystal Display

TTL- Transistor-Transistor Logic

GW- Gigawatt

MW- Megawatt

KW-Kilowatt

kWh- Kilowatt Hour

DC- Direct Current

AC- Alternating Current

GHG- Greenhouse Gas

SHS- Solar Home System

SREDA- Sustainable and Renewable Energy Development Authority

IDCOL- Infrastructure Development Company Limited

LED- Light Emitting Diode

FY- Fiscal Year

EE- Energy Efficiency

EC- Energy Conservation

M & C- Measurements and Characterization

λ- Wavelength

ν- Frequency

hν- Energy

eV- Electron Volt

q- Elementary Charge

c- Speed of light in vacuum

h- Planck's Constant

P(λ)- Spectral Power Density

Φ(λ)- Photon Flux Density

AM- Air Mass

Θ- Zenith Angle

μc-Si- Multi-crystalline

Eg- Bandgap

nm- Nanometer

DNI- Direct Normal Irradiation

E_V- Valence Band Edge

E_C- Conduction Band Edge

J_{sc}- Short Circuit Current Density

STC- Standard Test Condition

1 Chapter 1

Introduction

1.1 Introduction

Energy moves the modern world, available, reliable, affordable energy. Since the industrial revolution, fossil fuels (coal, oil, and natural gas) have powered immense technological progress. But supplies of fossil fuels are limited, and continued reliance on them may have significant environmental consequences. Fortunately, there are alternatives. The most powerful one is right over our heads. We are bathed in the clean, virtually inexhaustible energy of the sun. Each hour, enough sunlight reaches Earth to meet the world's energy needs for a year. To harvest this bounty, we need technology that efficiently converts the sun's energy into forms we can use. This is an exciting time for solar energy. Solar PV systems are being installed in unprecedented numbers worldwide [(1)]. Solar PV energy is widely available throughout the world and can contribute to reduced dependences on energy imports. As it entails no fuel price risk or constraints, it also improves security of supply. Solar power enhances energy diversity and hedges against price volatility of fossil fuels, thus stabilizing costs of electricity generation in the long term. Solar PV entails no greenhouse gas (GHG) emissions during operation and does not emit other pollutants (such as oxides of sulphur and nitrogen); additionally, it consumes no or little water. As local air pollution and extensive use of fresh water for cooling of thermal power plants are becoming serious concerns in hot or dry regions, these benefits of solar PV become increasingly important[(2)]. Solar PV is now one of the fast growing markets, meeting the worlds rapidly increasing energy demand, which is environmentally friendly and becoming more efficient and cost effective.

The year 2016 is going to mark the 62nd anniversary of the first public demonstration of a solar PV cell. On its 60th anniversary in 2014, solar PV markets around the world marked record year for growth, with about 40 GW of capacity added, for a global total of about 178 GW[3][4]. Global solar photovoltaic (PV) demand will reach 59 GW in 2015, an increase over the previous solar-PV demand forecast released in June 2015[5].The strong market in 2014 came despite the substantial decline in new installations in the European Union, challenges reaching targets (particularly for distributed systems) in China, and slower-than-expected emergence of promising new markets[6]More than 60% of all PV capacity in operation worldwide at the end of 2014 was added over the past three years[7] (See Figure[8] 1).

	TOTAL END-2013	ADDED 2014	TOTAL END-2014
		GW	
TOP COUNTRIES BY ADDITIONS			
China	17.5	10.6	28.2
Japan	13.6	9.7	23.3
United States	12.1	6.2	18.3
United Kingdom	3.4	2.4	5.2
Germany	36.3	1.9	38.2
France	4.7	0.9	5.7
Australia	3.2	0.9	4.1
South Korea	1.5	0.9	2.4
South Africa	0.1	0.8	0.9
India	2.5	0.7	3.2
TOP COUNTRIES BY TOTAL CAPACITY			
Germany	36.3	1.9	38.2
China	17.5	10.6	28.2
Japan	13.6	9.7	23.3
Italy	18.1	0.4	18.5
United States	12.1	6.2	18.3
France	4.7	0.9	5.7
Spain	5.3	~0	5.4
United Kingdom	2.8	2.4	5.2
Australia	3.2	0.9	4.1
India	2.5	0.7	3.2
World Total	**138**	**40**	**177**

Figure 1 Solar PV global capacity and additions, top 10 countries, 2014

We are in a state of ever increasing opportunity in the field of solar photovoltaic energy, with increasing jobs, markets worldwide and also in Bangladesh. But every technology first has to pass through some standardized tests and certification,

whether it is reliable, efficient and can help the user of that technology to ease their life. There exist some poor quality solar PV modules with relatively low cost. We need to test any system before install and check the performance characteristics. If the result is good we should go for it otherwise rejects to install these systems, which can be increase the cost and put us in a real fix. In this thesis, we are presenting a system capable of trace the I-V characteristics curve and analyze the curve to get the performance of solar PV modules in different weather conditions with respect to our climate.

1.2 Background

The generation of electrical power from a light source is known as photovoltaics and it is one of the most mainstream forms of renewable energy sources nowadays. Considering the country's future energy security, the Government has given priority to the implementation of renewable energy, energy efficiency as well as energy conservation programmes during the Sixth Plan (Five year plan). The Renewable Energy policy was approved in 2008. Through this policy the Government is committed to facilitate both public and private sector investment in renewable energy projects to substitute indigenous non- renewable energy supplies and scale up contributions of existing renewable energy based electricity productions. The Policy envisioned 5 percent of total generation from renewable sources by 2015 and 10 percent of the same by 2020. A nodal agency, the Sustainable and Renewable Energy Development Authority (SREDA), has been established and is expected to start working soon. Dedicated funding support has also been extended through government financial institutions like Bangladesh Bank and IDCOL as well as through private commercial banks. Moreover, Government has extended fiscal incentives including duty exemption on certain renewable energy products, e.g. solar panel, solar panel manufacturing accessories, LED light, solar operated light and wind power plant.

There is already some significant success in the area of solar energy that has delivered 150MW equivalent of power primarily through a highly successful Solar Home System (SHS) programme (Table 1). Some 3 million SHS units have been delivered. The Government's plan is to generate 800MW of power through renewable energy by FY2017 with a target of 10% of the total electricity to be met from renewable resources by FY2020.A special fund has been established to finance renewable energy based power plants. Some taka 4 billion was allocated to this Fund in FY2015.

The Government accorded high priority to the promotion of Energy Efficiency (EE) and Energy Conservation (EC) programmes during the Sixth Plan. The "Energy Efficiency and Conservation Map" and "Energy Efficiency Action Plan" have been prepared, and preparation of "Energy Efficiency and Conservation Master Plan" with support from Government of Japan is under process. Time-bound targets for energy savings have been set and programme implementation is well underway. The energy saving targets through the Energy Efficiency Action Plan and successful implementation of specific programmes will conserve resources. It will be a major step in implementing a sound energy strategy in Bangladesh [9].

Programme	Achievement
Solar Home System (SHS)	150 MW
Solar Irrigation	1 MW
Roof-top solar PV at Government buildings	14 MW
Wind energy	2 MW
Biomass based electricity	1 MW
Biogas based electricity	5 MW
Total	173 MW

Table 1Renewable energy progress during the sixth plan

1.2.1 Electricity through Renewable Energy (FY2016 to FY2020)

In view of the considerable challenge of primary fuel, the Seventh Plan (Five Year Plan- FY2016 to FY2020) recognizes that continued efforts will be needed to

accelerate the implementation of scalable power generation through renewable energy. This will be especially important to meet the demand in areas where grid supply is not possible during the Seventh Plan. The establishment of SREDA provides a strong dedicated institution to promote renewable energy. The Seventh plan will focus on two main areas of renewable energy: solar and wind power.

For the Seventh Plan the Government has adopted the 500WM Solar Programme broken down into 340MW of commercial purpose and 160MW of social sector. Commercial projects will be implemented by the private sector while social projects will be implemented by the different ministries and agencies as a part of social responsibility of the Government [9].Commercial projects are: (a) Solar Park (grid connected), (b) Solar Irrigation, (c) Solar Mini-grid/micro-grid and, (d) Solar rooftop. The social projects are: (a) Rural health centres, (b) Remote educational institutes, (c) Union e-Centres, (d) Remote Religious Establishment, (e) Off-grid Railway Stations and, (f) Government & Semi-Government Offices in the off-grid areas [10].

Bangladesh is completely dependent on imported solar PV modules and related accessories to meet her energy demand from solar power. In this regard a handful companies are involved in importing the panels and accessories and assembling. There must have some sort of testing and analyzing instruments and certification services to ensure reliable and efficient solar energy to user around the country. Here comes the need of a solar PV module performance characterization device, for both electrical characterization and for materials used. There are a lot of systems for measurement performance in worldwide. But we need this type of devices to be built in our country with our technology and along the climatic states being kept in mind. Tracing the I-V curve is one of the key indications to measure the electrical characteristics of a solar cell or module. By analyzing this I-V curve one can get the idea about the performance of a solar cell or module. This type of devices is needed in industries related to solar cell or module manufacturing and assembling along the certification and meeting the standards. Scientists and researchers also need this type of devices to enhance and improvement of solar PV systems.

We have developed a system that can measure the voltage and current a solar PV cell or module generates, when brings it to sunlight. After taking the current and voltage data we can analyze that data to get the electrical characteristics of that solar PV cell or module.

1.3 Literature Review

Worldwide in different academic institutions and in different organizations, they are working for innovation and development of solar PV module performance characterization analyzing tools. There exist a lot of systems already in markets and in the hand of many standardization organizations around the world. Here we are going to review some of the systems.

1.3.1 IV-Curve Plotter and Analyzer for Photovoltaic Module

The instrument is capable of tracing an IV characteristics curve of a solar module, using basic electronic devices like operational amplifier, transistors for the implementation of basic input and output manipulation and data acquisition from the PV panels. This instrument is an automatic calculator of the performance and quality parameters of Solar Module. This system used "Arduino Uno", a third party module for the programming and communication interface between the computer and the data acquiring circuits. Driving program has been developed using the Arduino Uno software. The instrument has been developed and tested in laboratory. Although there are some little fluctuations in the acquired data, the system can analyze the module characteristics property [11].

1.3.2 Novel Measuring System for Long Term Evaluation of Photovoltaic Modules

A new measurement technology for automated long term measurement evaluations of photovoltaic (PV) modules has been invented by IWES. The measuring card ISET-*mpp meter* not only allows the measurement of the main module parameters but also enables the complete I-V characteristics of the modules to be measured. Especially for newly developed modules this approach offers great potential for performance-tests, derivation of model parameters and new model equations. By using standardized communication commands it is possible to include the measuring board in a data acquisition system. Thus long-term measurements of PV modules in different operating modes and in different environments become possible. The I-V curves of the modules can be determined at specified intervals, or initiated by a trigger signal. Hereby for example, the influence of various weather conditions and shadowing situations to the module performance can be assessed. The measurement results can be sent via a serial port to a PC for further data processing [12].

1.3.3 The Model 4200-SCS Semiconductor Characterization System

Instrumentation such as the Model 4200-SCS Semiconductor Characterization System can simplify testing and analysis when making these critical electrical measurements. The Model 4200-SCS is an integrated system that includes instruments for making DC and ultra-fast I-V and C-V measurements, as well as control software, graphics, and mathematical analysis capability. The Model 4200-SCS is well-suited for performing a wide range of measurements, including DC and pulsed current-voltage (I-V), capacitance-voltage (C-V), capacitance-frequency (C-f), drive level capacitance profiling (DLCP), four-probe resistivity (ρ, σ), and Hall voltage (VH) measurements. This application note describes how to use the Model 4200-SCS to make these electrical measurements on PV cells. To simplify testing

photovoltaic materials and cells, the Model 4200-SCS is supported with a test project for making many of the mostly commonly used measurements easily. These tests, which include I-V, capacitance, and resistivity measurements, also include formulas for extracting common parameters such as the maximum power, short circuit current, defect density, etc. The *Solar Cell* project is included with all Model 4200-SCS systems running KTEI Version 8.0 or later. It provides thirteen tests in the form of ITMs (Interactive Test Modules) and UTMs (User Test Modules) for electrical characterization [13].

1.3.4 An Autonomous Online I-V Tracer for PV Monitoring Applications

This is a Solar PV modules I-V tracer, which operates autonomously, with no need to be disconnected from its load. The current state of I-V tracers commercially available will be discussed and motivation will be provided for the online autonomous I-V tracer. Design of such an I-V tracer using the single-ended primary inductance converter (SEPIC), and simulation results of such a converter operating as an I-V tracer presented. Analysis techniques of the I-V curve are also presented [14].

1.3.5 A Microcontroller-Based Data Acquisition System for Solar Radiation and Environmental Monitoring

The hardware design and operation of a battery powered microcontroller-based data acquisition system (herein referred to as the DAS) for unattended remote measurements are presented. The system was designed around the ST62E20 8-bit microcontroller and applied for solar radiation monitoring. The measurement system uses the Sol Data silicon-cell pyranometer as the solar radiation sensor. The

data from the sensor is collected by means of on-chip A/D converter and stored in a serial EEPROM until uploaded to a portable computer. Keeping the DAS in a low-power mode, which is only interrupted when measurements are to be taken or when a computer is connected to retrieve the stored data, minimizes power consumption. An on-chip timer provides an interrupt to awaken the system from its low-power wait mode at 10-min intervals to sample and store the data. At the end of each data collection period, the acquired data will be transmitted to the computer through the RS232 serial port for subsequent analysis. Only unprocessed data is stored in EEPROM. Quality control and data analysis is done off-line in the laboratory to minimize system cost, complexity and system downtime. Field tests and comparisons of this measurement system against the standard Eppley precision spectral pyranometer (PSP) have shown a slightly nonlinear correlation and that the accuracy of this measurement system as applied to solar radiation monitoring is fairly good, typically ±13W/m^{2}[15].

1.4 Objectives

Measurements and characterization (M&C) are vital to solar PV technology development. To verify progress, you need a way to measure it. To fix something, you need to know what's broken. Bangladesh is one of the countries, who are dependent on imported solar PV modules and accessories, as lack of technology growth in this field. So we need some sort of M & C system, made of our own to check those solar PV cells or modules and relevant accessories imported from the manufacturers. Technologies from other countries like M & C systems are expensive and when we need to get services from those product developers it adds an extra burden and kills valuable time of ours. In this regard we thought of a device which can help us to trace the I-V curve and analyze the electrical performance characteristics of those cells or modules in a reliable way. The main objectives of our thesis are as following

- To understand and observe the photovoltaic effect of converting light into electricity.
- To trace a current-voltage (I-V) characteristic curve of a solar PV cell or module.
- Store the I-V curve data collected form the panel into an erasable memory device.
- Collect data from the storage device and send it to an analyzing system or software.
- To develop an automatic diagnostic function of the photovoltaic modules based on the electrical characteristics of the solar PV cells or modules, which in terms, can provide information about the operational state of the system.
- Through the automatic diagnostic function, measure the maximum power point (MPP) , open circuit voltage (Voc), short circuit current (Isc), fill factor (FF), efficiency (η), temperature of the module (T) in °C, solar radiation or irradiance.
- To ensure a low cost I-V curve tracing and analyzing system for its user.

1.5 Thesis Outline

The thesis is organized in chapters, with sections within the chapters, and sub sections within the sections. These terms will be used throughout the text to refer to various portions of the document.

In Chapter 1, an introduction to recent solar photovoltaic power generation around the world with the emerging market has given. Motivation of our thesis presented in background section. Next two sections present the research objectives of our thesis and thesis outline.

Chapter 2 introduces the physics of a solar cell and its operation. It also explains the current voltage characteristic of the solar photovoltaic system. This chapter also introduces the components used in this project. Here the microcontroller (MC),

(MOSFET, USB to TTL serial converter, EEPROM, Liquid Crystal Display (LCD) etc. are being presented.

Chapter 3 deals with hardware and software development. Working circuit diagram and block diagram for the system are drawn along with the program flow diagram for the software and for MC programming. Programming codes for the systems are given in APPENDICES.

Chapter 4 describes the testing procedures and results of our project. We have tested our system and some snapshots of the system attached here. The I-V characteristics curve data and analyzed electrical performance characteristic data has presented in one of the section in this chapter.

Chapter 5 provides the conclusion and recommendation for future research and application of this project.

Several appendices are at the back of this thesis, and contain useful information for future students. Appendix A lists the formulas used in the text. Appendices B and C contains the programme of the microcontroller and the complete schematic diagram. Appendix D shows the board layout of the prototype printed circuit board used in testing.

2 Chapter 2

Theory and Familiarity of Components

2.1 Introduction

The sun delivers its energy to us in two main forms: heat and light. There are two main types of solar power systems, namely, solar thermal systems that trap heat to warm up water, and solar PV systems that convert sunlight directly into electricity. When the PV modules are exposed to sunlight, they generate direct current ("DC") electricity. An inverter then converts the DC into alternating current ("AC") electricity, so that it can feed into one of the building's AC distribution boards ("ACDB") without affecting the quality of power supply[16].The basic element of a PV system is the PV solar cell that converts solar energy into direct-current (DC) electricity. PV cells are assembled and electrically interconnected to form PV modules. Several PV modules are connected in a series and/or in parallel to increase voltage and/or current, respectively. An inverter is needed to convert DC into AC for grid integration and use with most electrical appliances. Modules and balance of system (i.e. inverter, racking, power control, cabling and batteries, if any) form a modular PV system with a capacity ranging from a few kW to virtually hundreds of MW. PV systems can be integrated into building structures (i.e. building-adaptive or integrated PV systems, BAPV or BIPV), placed on roofs or ground-based. A number of PV technologies are either commercially available or under development. They can be grouped into three categories that are also referred to as 1st, 2nd and 3rd generation: 1) wafer-based crystalline silicon (**c-Si**); 2) thin-films (**TF**); and 3) emerging and novel PV technologies, including concentrating PV, organic PV, advanced thin films and other novel concepts. Over the past two decades, PV

technologies have dramatically improved their performance (i.e. efficiency, lifetime, energy pay-back time) and reduced their costs, and this trend is expected to continue in the future. Research aims to increase efficiency and lifetime, as well as reduce the investment costs so as to minimize the electricity generation cost. Several studies have analyzed the development of PV performance and costs over time [17].

2.2 Solar Radiation

The solar radiation is attenuated, when it passes through the earth's atmosphere. Since the spectral distribution of the solar radiation also depends on the attenuation, various solar spectra can be measured at the earth's surface. The degree of attenuation is variable. The most important parameter that determines the solar irradiance under clear sky conditions is the distance that the sunlight has to travel through the atmosphere. This distance is the shortest when the sun is at the zenith, i.e. directly overhead. The ratio of an actual path length of the sunlight to this minimal distance is known as the *optical air mass*. When the sun is at its zenith the optical air mass is unity and the radiation is described as *air mass one* (AM1) radiation. When the sun is at an angle θ to the zenith, the air mass is given by

$$\text{Air mass} = (\text{Cos}\theta)^{-1} \qquad 2.1$$

The spectral power density of some commonly used air mass radiation spectra are presented in Figure 6. AM0 radiation is the extraterrestrial spectrum of solar radiation outside the earth's atmosphere, which power density is the solar constant. Opposed to the situation outside the earth's atmosphere, terrestrial solar radiation varies both in intensity and spectral distribution depending on the position on the earth and the position of the sun in the sky. In order to allow comparison between the performances of solar cells tested at different locations, a terrestrial solar radiation standard has to be defined and measurements referred to this standard. *AM1.5radiation* serves at present as the standard spectral distribution. It corresponds to an angle of 48.2 degrees between the sun's position and the zenith.

The irradiance of the AM1.5 radiation is 827 W/m^2. The value of 1000 W/m^2 was incorporated to become a standard. This value of the irradiance is close to the maximum received at the earth's surface. The peak power of a photovoltaic system is the power generated under this standard AM1.5 (1000 W/m^2) radiation and is expressed in peak watts.

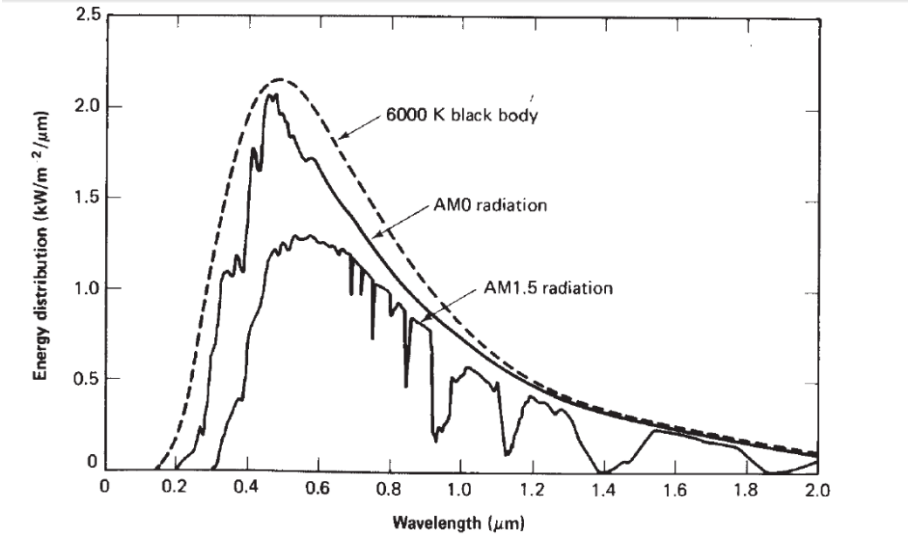

Figure 2 Spectral power density of sunlight. The different spectra refer to the black-body

The design of an optimal photovoltaic system for a particular location depends on the availability of the solar insolation data at the location. Solar irradiance integrated over a period of time is called solar irradiation. For example, the average annual solar irradiation in The Netherlands is 1000 kWh/ m^2, while in Sahara the average value is 2200 kWh/ m^2.The presently accepted value of the solar constant in photovoltaic work is 1.353kWm^{-2}. This value has been determined by taking a weighted average of measurements made by equipment mounted on balloons, high altitude aircraft, and spacecraft [18]. As indicated by the two uppermost curves in figure 2, the spectral distribution of AM0 radiation differs from that of an ideal black body. This is due to such effects as differing transmissivity of the sun's atmosphere at different wavelengths. Knowledge of the exact distribution of the energy content in sunlight is important in solar cell work because these cells respond differently to different wavelengths of light [19].

2.3 The Working Principle of a Solar Cell

The working principle of solar cells is based on the photovoltaic effect, i.e. the generation of a potential difference at the junction of two different materials in response to electromagnetic radiation. The photovoltaic effect is closely related to the photoelectric effect, where electrons are emitted from a material that has absorbed light with a frequency above a material-dependent threshold frequency. In 1905, Albert Einstein understood that this effect can be explained by assuming that the light consists of well-defined energy quanta, called photons. The energy of such a photon is given by

$$E=h\nu \qquad 2.2$$

Where h is Planck's constant and ν is the frequency of the light. For his explanation of the photoelectric effect Einstein received the Nobel Prize in Physics in 1921[20].

The photovoltaic effect can be divided into three basic processes:

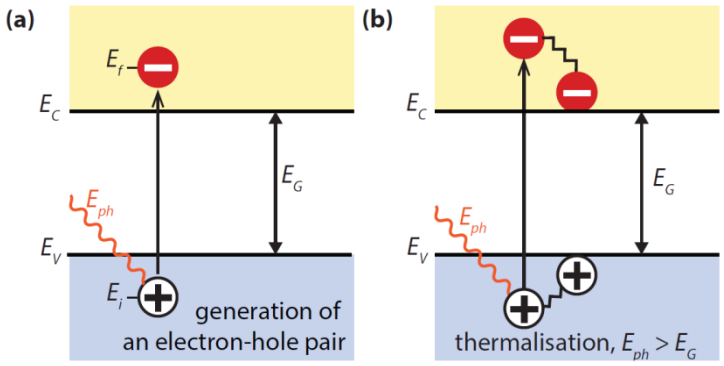

Figure 3 (a) Illustrating the absorption of a photon in a semiconductor with band gap Eg. The photon with energy Eph = hν excites an electron from Ei to Ef . At Ei a hole is created. (b) If Eph>Eg, a part of the energy is thermalised.

1. Generation of charge carriers due to the absorption of photons in the materials that form a junction.

Absorption of a photon in a material means that its energy is used to excite an electron from an initial energy level Ei to a higher energy level Ef, as shown in Fig.

3(a). Photons can only be absorbed if electron energy levels Ei and Ef are present so that their difference equals to the photon energy, hν = Ef - Ei. In an ideal semiconductor electrons can populate energy levels below the so-called valence band edge, E_V, and above the so called conduction band edge, E_C. Between those two bands no allowed energy states exist, which could be populated by electrons. Hence, this energy difference is called the bandgap, Eg = E_C - E_V. If a photon with energy smaller than Eg reaches an ideal semiconductor, it will not be absorbed but will traverse the material without interaction.

In a real semiconductor, the valence and conduction bands are not flat, but vary depending on the so-called k-vector that describes the crystal momentum of the semiconductor. If the maximum of the valence band and the minimum of the conduction band occur at the same k-vector, an electron can be excited from the valence to the conduction band without a change in the crystal momentum. Such a semiconductor is called a direct bandgap material. If the electron cannot be excited without changing the crystal momentum, we speak of an indirect bandgap material. The absorption coefficient in a direct bandgap material is much higher than in an indirect bandgap material, thus the absorber can be much thinner [21]. If an electron is excited from Ei to Ef, a void is created at Ei. This void behaves like a particle with a positive elementary charge and is called a hole. The absorption of a photon therefore leads to the creation of an electron-hole pair, as illustrated in Figure4 (**1**). The radiative energy of the photon is converted to the chemical energy of the electron-hole pair. The maximal conversion efficiency from radiative energy to chemical energy is limited by thermodynamics. This thermodynamic limit lies in between 67% for non-concentrated sunlight and86% for fully concentrated sunlight [22].

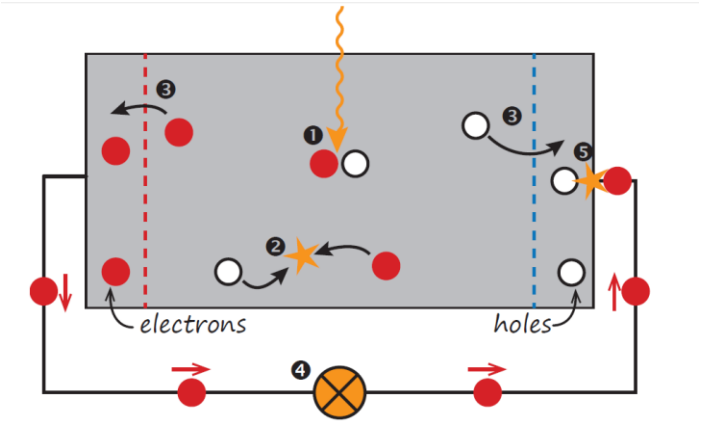

Figure 4 A very simple solar cell model. (**1**) Absorption of a photon leads to the generation of an electron-hole pair. (**2**) Usually, the electrons and holes will combine. (**3**) With semipermeable membranes the electrons and the holes can be separated. (**4**) The separated electrons can be used to drive an electric circuit. (**5**) After the electrons passed through the circuit, they will recombine with holes

2. Subsequent separation of the photo-generated charge carriers in the junction.

Usually, the electron-hole pair will recombine, i.e. the electron will fall back to the initial energy level Ei, as illustrated in Figure 4 (**2**). The energy will then be released either as photon (radiative recombination) or transferred to other electrons or holes or lattice vibrations (non radiative recombination). If one wants to use the energy stored in the electron-hole pair for performing work in an external circuit, semipermeable membranes must be present on both sides of the absorber, such that electrons only can flow out through one membrane and holes only can flow out through the other membrane[22], as illustrated in Figure 4 (**3**). In most solar cells, these membranes are formed by n- and p-type materials.

A solar cell has to be designed such that the electrons and holes can reach the membranes before they recombine, i.e. the time it requires the charge carriers to reach the membranes must be shorter than their lifetime. This requirement limits the thickness of the absorber.

3. Collection of the photo-generated charge carriers at the terminals of the junction.

Finally, the charge carriers are extracted from the solar cells with electrical contacts so that they can perform work in an external circuit (Figure 4 (**4**)). The chemical energy of the electron-hole pairs is finally converted to electric energy. After the electrons passed through the circuit, they will recombine with holes at a metal absorber interface, as illustrated in Figure 4 (**5**).

2.4 The I-V Characteristic Curve

The current-voltage (I-V) curve of a non-shadowed PV module has three remarkable points – the maximum-power point (MPP), short circuit and open circuit. A photovoltaic module will produce its maximum current when there is essentially no resistance in the circuit. This would be a short circuit between its positive and negative terminals [23].

Example

From the graph given below, I_{sc} = 2.65 A, V_{oc} = 21.3 V, At MPP, I_{mp} = 2.5 A, V_{mp}= 17.3V =>Pmp= 2.5 x 17.3 = 43.25 W, The optimal resistance for operation = V_{mp}/ I_{mp} = 17.3/2.5 = 6.9 ohms

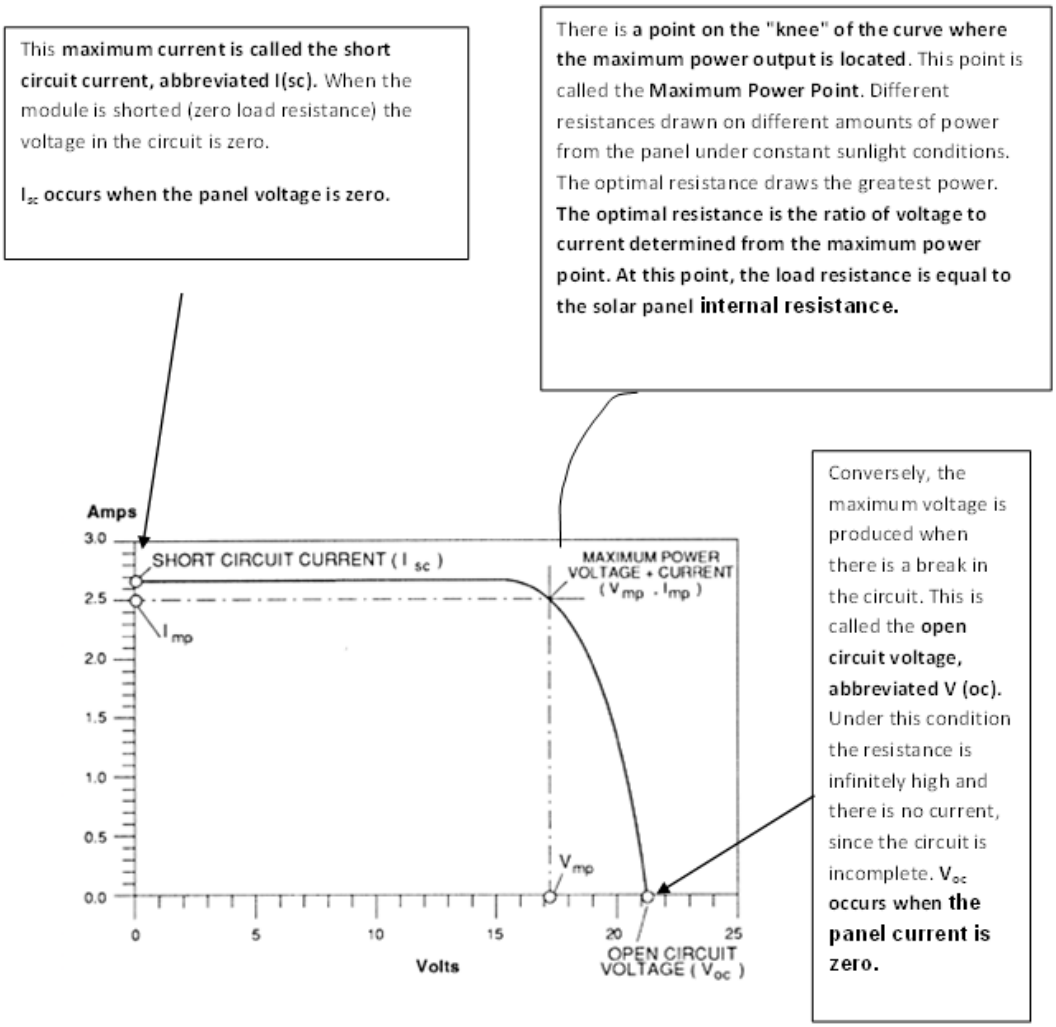

Figure 5 Illustration of I-V Characteristic Curve of a PV Module

The equivalent circuit shown in Figure 5 and described by Equation 2.3 represents a PV cell [24].

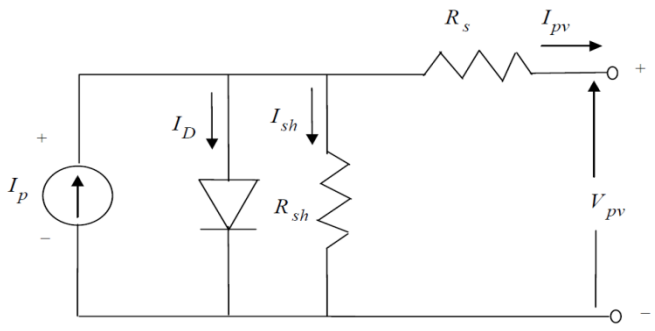

Figure 6 Equivalent circuit of a PV cell

$$I_{pv} = I_p - I_D - I_{sh} = I_p - I_o \left(e^{\frac{q\,(V_{pv}+R_s\,I_{pv})}{NKT}} - 1\right) - \frac{V_{pv}+R_s\,I_{pv}}{R_{sh}} \qquad 2.3$$

Where, I_p= Photocurrent [A], V_{pv}= Terminal voltage of the cell [V], I_D= Diode current [A], I_o= Saturation current [A], I_{sh}= Shunt current [A], N = Ideality factor, Q = Electron charge [C], k = Boltzmann's constant, T = Junction temperature [K], R_s= Series resistance [Ω], R_{sh}= Shunt resistance [Ω].

2.4.1 Short-Circuit Current

The short-circuit current is the current through the solar cell when the voltage across the solar cell is zero (i.e., when the solar cell is short circuited). Usually written as I_{SC}, the short-circuit current is shown on the IV curve below.

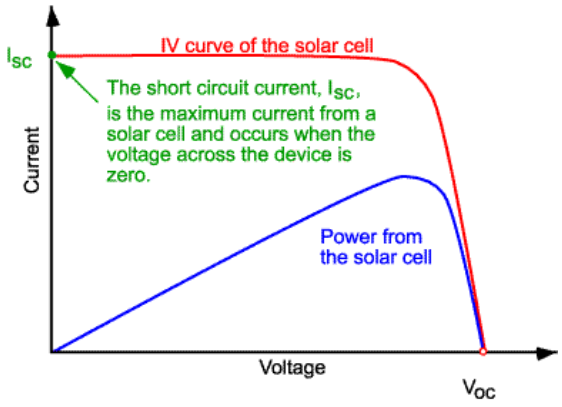

Figure 7 I-V curve of a solar cell showing the short-circuit current

The short-circuit current is due to the generation and collection of light-generated carriers. For an ideal solar cell, at most moderate resistive loss mechanisms, the short circuit current and the light-generated current are identical. Therefore, the short-circuit current is the largest current which may be drawn from the solar cell.

The short-circuit current depends on a number of factors which are described below:

- The area of the solar cell. To remove the dependence of the solar cell area, it is more common to list the short-circuit current density (J_{sc} in mA/cm^2) rather than the short-circuit current;
- The number of photons (i.e., the power of the incident light source). I_{sc} from a solar cell is directly dependent on the light intensity as discussed in Effect of Light Intensity;
- The spectrum of the incident light. For most solar cell measurement, the spectrum is standardised to the AM1.5 spectrum;
- The optical properties (absorption and reflection) of the solar cell; and
- The collection probability of the solar cell, which depends chiefly on the surface passivation and the minority carrier lifetime in the base.

When comparing solar cells of the same material type, the most critical material parameter is the diffusion length and surface passivation. In a cell with perfectly passivated surface and uniform generation, the equation for the short-circuit current can be approximated as:

$$J_{sc} = qG\,(L_n + L_p) \qquad 2.4$$

Where G is the generation rate, and L_n and L_p are the electron and hole diffusion lengths respectively. Although this equation makes several assumptions which are not true for the conditions encountered in most solar cells, the above equation nevertheless indicates that the short-circuit current depends strongly on the generation rate and the diffusion length.

2.4.1.1 Illuminated Current and Short Circuit Current (IL or Isc?)

I_L is the light generated current inside the solar cell and is the correct term to use in the solar cell equation. At short circuit conditions the externally measured current is $I_{sc.}$ Since I_{sc} is usually equal to I_L, the two are used interchangeably and for simplicity and the solar cell equation is written with I_{sc} in place of I_L. In the case of very high

series resistance (> 10 Ωcm^2) I_{sc} is less than I_L and writing the solar cell equation with I_{sc} is incorrect.

Another assumption is that the illumination current I_L is solely dependent on the incoming light and is independent of voltage across the cell. However, I_L varies with voltage in the case of drift-field solar cells and where carrier lifetime is a function of injection level such as defected multicrystalline materials [25].

2.4.2 Open-Circuit Voltage

The open-circuit voltage, V_{OC}, is the maximum voltage available from a solar cell, and this occurs at zero current. The open-circuit voltage corresponds to the amount of forward bias on the solar cell due to the bias of the solar cell junction with the light-generated current. The open-circuit voltage is shown on the IV curve below.

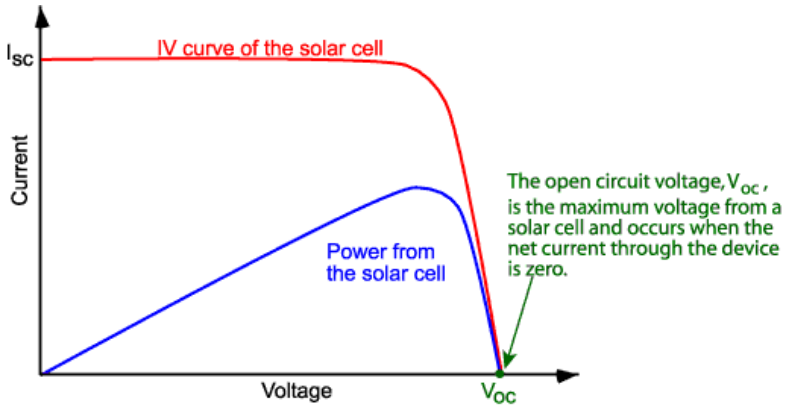

Figure 8 I-V curve of a solar cell showing the open-circuit voltage

An equation for V_{oc} is found by setting the net current equal to zero in the solar cell equation to give:

$$V_{OC} = \frac{nkT}{q} \ln\left(\frac{I_L}{I_o} + 1\right) \qquad 2.5$$

The above equation shows that V_{oc} depends on the saturation current of the solar cell and the light-generated current. While I_{sc} typically has a small variation, the key effect is the saturation current, since this may vary by orders of magnitude. The saturation current, I_0 depends on recombination in the solar cell. Open-circuit voltage is then a measure of the amount of recombination in the device. Silicon solar cells on high quality single crystalline material have open-circuit voltages of up to 730 mV under one sun and AM1.5 conditions, while commercial devices on multicrystalline silicon typically have open-circuit voltages around 600 mV.

The V_{OC} can also be determined from the carrier concentration [26]:

$$V_{OC} = \frac{kT}{q} \ln \left[\frac{(N_A + \Delta n)\Delta n}{n_i^2} \right] \qquad 2.6$$

Where kT/q is the thermal voltage, N_A is the doping concentration, Δn is the excess carrier concentration and n_i is the intrinsic carrier concentration. The determination of V_{OC} from the carrier concentration is also termed Implied V_{OC}.

2.4.3 Irradiation effect

Photovoltaic output power is affected by incident irradiation. PV module short circuit current (I_{sc}) is linearly proportional to the irradiation, while open circuit voltage (V_{oc}) increases exponentially to the maximum value with increasing the incident irradiation, and it varies slightly with the light intensity[27]. Figure 9 describes the relation between Photovoltaic voltage and current with the incident irradiation.

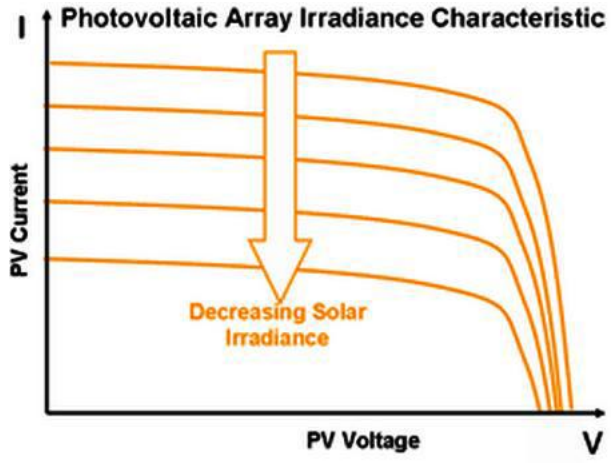

Figure 9 Effects of the incident irradiation on module voltage and current [27]

2.4.4 Temperature effect

Module temperature is highly affected by ambient temperature. Short circuit current increases slightly when the PV module temperature increases more than the Standard Test Condition (STC) temperature, which is 25°C. However, open circuit voltage is enormously affected when the module temperature exceeds 25°C. In other words the increasing current is proportionally lower than the decreasing voltage. Therefore, the output power of the PV module is reduced [27]. Figure 10 explains the relation between module temperature with voltage and current.

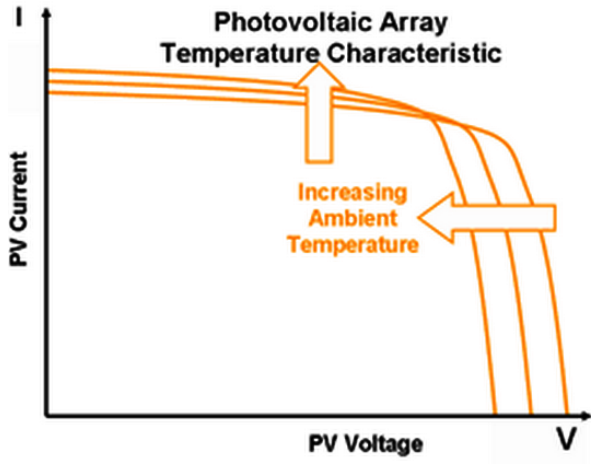

Figure 10 Effect of ambient temperature on module voltage and current [27]

2.4.5 Maximum power point (P_{MPP})

Maximum electrical power of the PV module is equal to the current at maximum power point (IMP) multiplied by the voltage at maximum power point (VMP), which is the maximum possible power at Standard Test Condition (STC). Referring to Figure 11, the “knee” of the I-V curve represents the maximum power point (PMPP) of the PV module/system. At this point the maximum electrical power is generated at STC [28].The usable electrical output power depends on the PV module efficiency which is related to the module technology and manufacture.

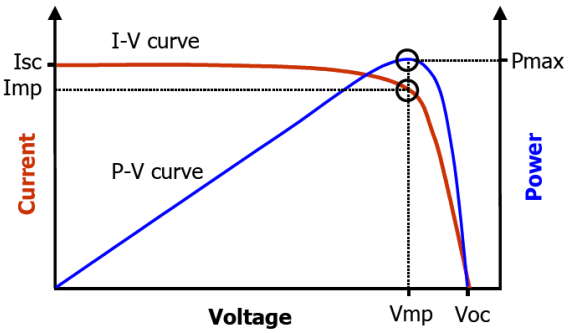

Figure 11 Maximum power point [28]

2.4.6 Fill factor (FF)

The short-circuit current and the open-circuit voltage are the maximum current and voltage respectively from a solar cell. However, at both of these operating points, the power from the solar cell is zero. The "fill factor", more commonly known by its abbreviation "FF", is a parameter which, in conjunction with V_{oc} and I_{sc}, determines the maximum power from a solar cell. The FF is defined as the ratio of the maximum power from the solar cell to the product of V_{oc} and I_{sc}. Graphically, the FF is a measure of the "squareness" of the solar cell and is also the area of the largest rectangle which will fit in the IV curve. The FF is illustrated below.

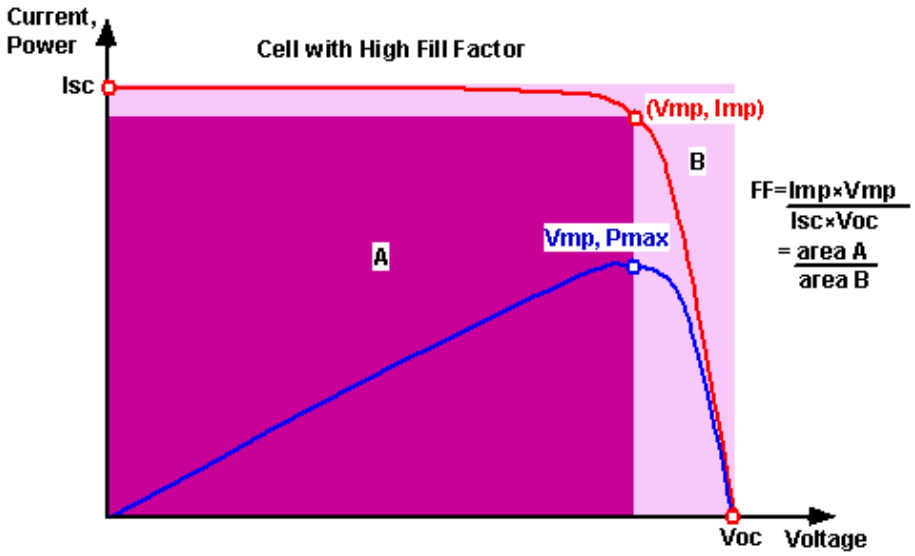

Figure 12 Graph of cell output current (red line) and power (blue line) as function of voltage. Also shown are the cell short-circuit current (Isc) and open-circuit voltage (Voc) points, as well as the maximum power point (Vmp, Imp)

As FF is a measure of the "squareness" of the IV curve, a solar cell with a higher voltage has a larger possible FF since the "rounded" portion of the IV curve takes up less area. The maximum theoretical FF from a solar cell can be determined by differentiating the power from a solar cell with respect to voltage and finding where this is equal to zero [29]. FF is most commonly determined from measurement of the IV curve and is defined as the maximum power divided by the product of I_{sc}*V_{oc}, i.e.:

$$FF = \frac{V_{MP} I_{MP}}{V_{OC} I_{SC}} \qquad 2.7$$

2.4.7 Efficiency

The efficiency is the most commonly used parameter to compare the performance of one solar cell to another. Efficiency is defined as the ratio of energy output from the solar cell to input energy from the sun. In addition to reflecting the performance of the solar cell itself, the efficiency depends on the spectrum and intensity of the incident sunlight and the temperature of the solar cell. Therefore, conditions under which efficiency is measured must be carefully controlled in order to compare the

performance of one device to another. Terrestrial solar cells are measured under AM1.5 conditions and at a temperature of 25°C. Solar cells intended for space use are measured under AM0 conditions [30].

The efficiency of a solar cell is determined as the fraction of incident power which is converted to electricity and is defined as:

$$P_{max} = V_{OC} I_{SC} FF \tag{2.8}$$

$$\eta = \frac{V_{OC} I_{SC} FF}{P_{in}} \tag{2.9}$$

Where V_{oc} is the open-circuit voltage; I_{sc} is the short-circuit current; and FF is the fill factor, η is the efficiency.

The input power for efficiency calculations is 1 kW/m^2 or 100mW/cm^2. Thus the input power for a 100 × 100 mm^2 cell is 10 W and for a 156 × 156 mm^2 cell is 24.3 W.

2.4.8 Shunt Resistance

Significant power losses caused by the presence of a shunt resistance, R_{SH}, are typically due to manufacturing defects, rather than poor solar cell design. Low shunt resistance causes power losses in solar cells by providing an alternate current path for the light generated current. Such a diversion reduces the amount of current flowing through the solar cell junction and reduces the voltage from the solar cell. The effect of a shunt resistance is particularly severe at low light levels, since there will be less light generated current. The loss of this current to the shunt therefore has a larger impact. In addition, at lower voltages where the effective resistance of the solar cell is high, the impact of a resistance in parallel is large [31].

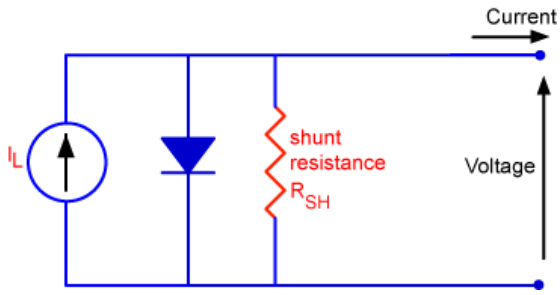

Figure 13 Circuit diagram of a solar cell including the shunt resistance

The equation for a solar cell in presence of a shunt resistance is:

$$I=I_L-I_0\exp[qVnkT]-VR_{SH} \qquad 2.10$$

Where, I is the cell output current, I_L is the light generated current, V is the voltage across the cell terminals, T is the temperature, q and k are constants, n is the ideality factor, and R_{SH} is the cell shunt resistance.

2.4.9 Series Resistance

Series resistance in a solar cell has three causes: firstly, the movement of current through the emitter and base of the solar cell; secondly, the contact resistance between the metal contact and the silicon; and finally the resistance of the top and rear metal contacts. The main impact of series resistance is to reduce the fill factor, although excessively high values may also reduce the short-circuit current.

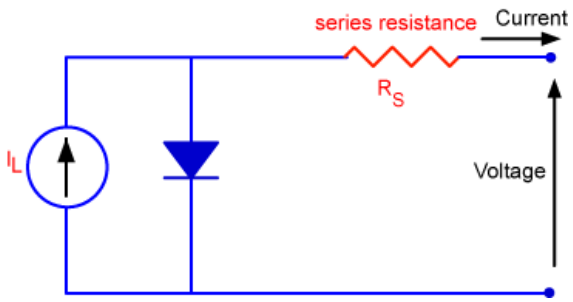

Figure 14 Schematic of a solar cell with series resistance

$$I=I_L-I_0 \exp[q(V+IR_S)/nkT] \quad 2.11$$

Where: I is the cell output current, I_L is the light generated current, V is the voltage across the cell terminals, T is the temperature, q and k are constants, n is the ideality factor, and R_S is the cell series resistance. The formula is an example of an implicit function due to the appearance of the current, I, on both sides of the equation and requires numerical methods to solve.

2.5 Familiarity of Components

2.5.1 Temperature Sensor (LM35)

The LM35 series are precision integrated-circuit temperature sensors, whose output voltage is linearly proportional to the Celsius (Centigrade) temperature. The LM35 thus has an advantage over linear temperature sensors calibrated in °Kelvin, as the user is not required to subtract a large constant voltage from its output to obtain convenient Centigrade scaling. The LM35 does not require any external calibration or trimming to provide typical accuracies of ±1/4°C at room temperature and ±3/4°C cover a full −55 to +150°C temperature range. Low cost is assured by trimming and calibration at the wafer level. The LM35's low output impedance, linear output, and precise inherent calibration make interfacing to readout or control circuitry especially easy. It can be used with single power supplies, or with plus and minus supplies.

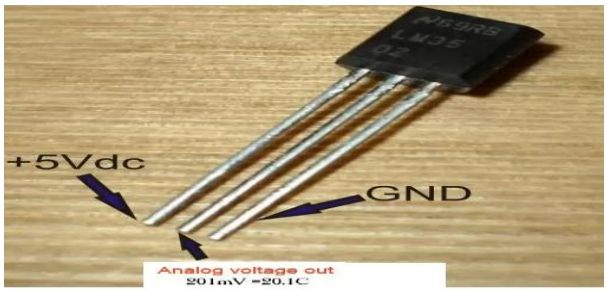

Figure 15 Temperature Sensor (LM35DZ)

2.5.2 Positive-Voltage Regulator (Lm7805)

This series of fixed-voltage integrated-circuit voltage regulators is designed for a wide range of applications. These applications include on-card regulation for elimination of noise and distribution problems associated with single-point regulation. Each of these regulators can deliver up to 1.5 A of output current. The internal current-limiting and thermal-shutdown features of these regulators essentially make them immune to overload. In addition to use as fixed-voltage regulators, these devices can be used with external components to obtain adjustable output voltages and currents, and also can be used as the power-pass element in precision regulators.

Features of LM7805

- 3-Terminal Regulators with Output Current up to 1.5 A
- Internal Thermal-Overload Protection
- High Power-Dissipation Capability
- Internal Short-Circuit Current Limiting
- Output Transistor Safe-Area Compensation

2.5.3 Power MOSFET (RFP70N06)

N-Channel Power MOSFET of 60V, 70A, 14mΩ is selected. These are N-Channel power MOSFETs manufactured using the MegaFET process. This process, which uses feature sizes approaching those of LSI circuits, gives optimum utilization of silicon, resulting in outstanding performance. They were designed for use in applications such as switching regulators, switching converters, motor drivers and relay drivers. These transistors can be operated directly from integrated circuits.

Figure 16 N-Channel Power MOSFET RFP70N06

Features

- 70A, 60V
- $r_{DS}(on)$ = 0.014Ω
- Temperature Compensated PSPICE® Model
- Peak Current vs. Pulse Width Curve
- UIS Rating Curve (Single Pulse)
- 175 o C Operating Temperature

2.5.4 Photocoupler (TLP250)

The TLP250 consists of a GaAlAs light emitting diode and a integrated photodetector. This unit is 8–lead DIP package. TLP250 is suitable for gate driving circuit of IGBT or power MOSFET.

Features of TLP250

- Input threshold current IF=5mA(max.)
- Supply current (ICC) 11mA(max.)
- Supply voltage (VCC) 10–35V
- Output current (IO) ±1.5A (max.)
- Switching time (tpLH/tpHL) 1.5μs(max.)
- Isolation voltage 2500Vrms(min.)

2.5.5 USB-TTL Interface Module

The USB-TTL Interface Module (for brevity, Module hereafter) can be used to add USB connectivity to any microcontroller or other device that is capable of standard serial communication. There are several configuration options on the Module that facilitate its use in a variety of situations. The Module can be powered from the USB hub or from an external supply.

When powered by the USB hub, the Module can optionally provide power to external circuitry. The Module can be configured for either a 5 volt or a 3.3 volt signal interface and it can provide 3.3 volt power to external circuitry as well, subject to current limits.

Figure 17 USB to TTL Interface Module

2.5.6 Two-wire Serial EEPROM (AT24C512B)

The AT24C512B provides 524,288 bits of serial electrically erasable and programmable read only memory (EEPROM) organized as 65,536 words of 8 bits each. The device's cascadable feature allows up to eight devices to share a common two-wire bus. The device is optimized for use in many industrial and commercial applications where low-power and low-voltage operation are essential. The devices are available in space-saving 8-pin PDIP, 8-lead JEDEC SOIC, 8-lead EIAJ SOIC, 8-lead TSSOP, 8-ball dBGA2 and 8-lead Ultra-Thin SAP packages. In addition, the entire family is available in 1.8V (1.8V to 3.6V) and 2.5V (2.5V to 5.5V) versions.

Pin Description

SERIAL CLOCK (SCL) The SCL input is used to positive edge clock data into each EEPROM device and negative edge clock data out of each device.

SERIAL DATA (SDA) The SDA pin is bidirectional for serial data transfer. This pin is open drain driven and may be wire-ORed with any number of other open-drain or open collector devices.

DEVICE/PAGE ADDRESSES (A2, A1, A0) The A2, A1, and A0 pins are device address inputs that are hardwired (directly to GND or to Vcc) for compatibility with other AT24Cxx devices. When the pins are hardwired, as many as eight 512K devices may be addressed on a single bus system. A device is selected when a corresponding hardware and software match is true. If these pins are left floating, the A2, A1, and A0 pins will be internally pulled down to GND.

WRITE PROTECT (WP) The write protect input, when connected to GND, allows normal write operations. When WP is connected directly to Vcc, all write operations to the memory are inhibited. If the pin is left floating, the WP pin will be internally pulled down to GND.

Device Operation

Clock and Data Transitions, the SDA pin is normally pulled high with an external device. Data on the SDA pin may change only during SCL low time periods. Data changes during SCL high periods will indicate a start or stop condition as defined below.

Start Condition A high-to-low transition of SDA with SCL high is a start condition which must precede any other command.

Stop Condition A low-to-high transition of SDA with SCL high is a stop condition. After a read sequence, the stop command will place the EEPROM in a standby power mode.

Acknowledge All addresses and data words are serially transmitted to and from the EEPROM in 8-bit words. The EEPROM sends a zero during the ninth clock cycle to acknowledge that it has received each word.

Standby Mode the AT24C512B features a low power standby mode which is enabled: a) upon power-up and b) after the receipt of the STOP bit and the completion of any internal operations.

Software Reset After an interruption in protocol, power loss or system reset, any 2-wire part can be protocol reset by following these steps: (a) Create a start bit condition, (b) clock 9 cycles, (c) Create another start bit followed by stop bit condition.

Features of AT24C512B

• Low-voltage/Standard-voltage Operation: 1.8v (VCC = 1.8V to 3.6V), 2.5v (VCC = 2.5V to 5.5V)
• Two-wire Serial Interface, Schmitt Triggers, Filtered Inputs for Noise Suppression
• Bidirectional Data Transfer Protocol
• 1 MHz (2.5V, 5.5V), 400 kHz (1.8V) Compatibility

• 128-byte Page Write Mode (Partial Page Writes Allowed)
• Self-timed Write Cycle (5 ms Max)
• High Reliability: Endurance: 1,000,000 Write Cycles, Data Retention: 40 Years

2.5.7 Microcontroller

Micro suggests that the device is small, and *controller* means the device might be used to control objects, processes, or events. Another term to describe a microcontroller is *embedded controller*, because the microcontroller and its support circuits are often built into, or embedded in, the devices they control. Soa Microcontroller (MCU) is a device which integrates a number of components (microprocessor, RAM, ROM, I/O) of a microprocessor system onto a single microchip. That is, a MCU combines onto a same microchip: 1. The CPU core, 2. Memory (both RAM and ROM) and 3. Some parallel digital I/O and others

2.5.7.1 Needs of Microcontroller

- Low cost ,small packaging
- Low power consumption
- Programmable , re-programmable
- Lots of I/O capabilities
- Easy integration with circuits
- For applications in which cost , power and space are critical
- Single-purpose

2.5.7.2 ATMEGA32Device Overview

The Atmel®AVR®ATmega32 is a low-power CMOS 8-bit microcontroller based on the AVR enhanced RISC architecture. By executing powerful instructions in a single

clock cycle, the ATmega32 achieves throughputs approaching 1 MIPS per MHz allowing the system designer to optimize power consumption versus processing speed.

Pin Descriptions

VCC Digital supply voltage.

GNDGround.

Port A (PA7..PA0) Port A serves as the analog inputs to the A/D Converter. Port A also serves as an 8-bit bi-directional I/O port, if the A/D Converter is not used. Port pins can provide internal pull-up resistors (selected for each bit). The Port A output buffers have symmetrical drive characteristics with both high sink and source capability. When pins PA0 to PA7 are used as inputs and are externally pulled low, they will source current if the internal pull-up resistors are activated. The Port A pins are tri-stated when a reset condition becomes active, even if the clock is not running.

Port B (PB7..PB0) Port B is an 8-bit bi-directional I/O port with internal pull-up resistors (selected for each bit). The Port B output buffers have symmetrical drive characteristics with both high sink and source capability. As inputs, Port B pins that are externally pulled low will source current if the pull-up resistors are activated. The Port B pins are tri-stated when a reset condition becomes active, even if the clock is not running. Port B also serves the functions of various special features of the ATmega32.

Port C (PC7..PC0) Port C is an 8-bit bi-directional I/O port with internal pull-up resistors (selected for each bit). The Port C output buffers have symmetrical drive characteristics with both high sink and source capability. As inputs, Port C pins that are externally pulled low will source current if the pull-up resistors are activated. The Port C pins are tri-stated when a reset condition becomes active, even if the clock is not running. If the JTAG interface is enabled, the pull-up resistors on pins PC5(TDI), PC3(TMS) and PC2(TCK) will be activated even if a reset occurs. The TD0

pin is tri-stated unless TAP states that shift out data are entered. Port C also serves the functions of the JTAG interface and other special features of the ATmega32.

Port D (PD7..PD0) Port D is an 8-bit bi-directional I/O port with internal pull-up resistors (selected for each bit). The Port D output buffers have symmetrical drive characteristics with both high sink and source capability. As inputs, Port D pins that are externally pulled low will source current if the pull-up resistors are activated. The Port D pins are tri-stated when a reset condition becomes active, even if the clock is not running.

RESET is use to Reset Input. A low level on this pin for longer than the minimum pulse length will generate a reset, even if the clock is not running. Shorter pulses are not guaranteed to generate a reset.

XTAL1 Input to the inverting Oscillator amplifier and input to the internal clock operating circuit.

XTAL2 Output from the inverting Oscillator amplifier.

AVCC is the supply voltage pin for Port A and the A/D Converter. It should be externally connected to VCC, even if the ADC is not used. If the ADC is used, it should be connected to VCC through a low-pass filter.

AREF is the analog reference pin for the A/D Converter.

Features of ATMEGA32

High Endurance Non-volatile Memory Segments

- 32Kbytes of In-System Self-programmable Flash program memory
- 1024Bytes EEPROM, 2K bytes Internal SRAM
- Write/Erase Cycles: 10,000 Flash/100,000 EEPROM
- Data retention: 20 years at 85°C/100 years at 25°C(1)

Peripheral Features

- Two 8-bit Timer/Counters with Separate Prescalers and Compare Modes
- One 16-bit Timer/Counter with Separate Prescaler, Compare Mode, and Capture Mode
- Real Time Counter with Separate Oscillator

- Four PWM Channels
- 8-channel, 10-bit ADC
  - 8 Single-ended Channels
  - 7 Differential Channels in TQFP Package Only
  - 2 Differential Channels with Programmable Gain at 1x, 10x, or 200x
- Byte-oriented Two-wire Serial Interface

Special Microcontroller Features

- Power-on Reset and Programmable Brown-out Detection
- Internal Calibrated RC Oscillator
- External and Internal Interrupt Sources
- Six Sleep Modes: Idle, ADC Noise Reduction, Power-save, Power-down, Standby and Extended Standby

2.5.7.3 Atmel AVR Core Architecture

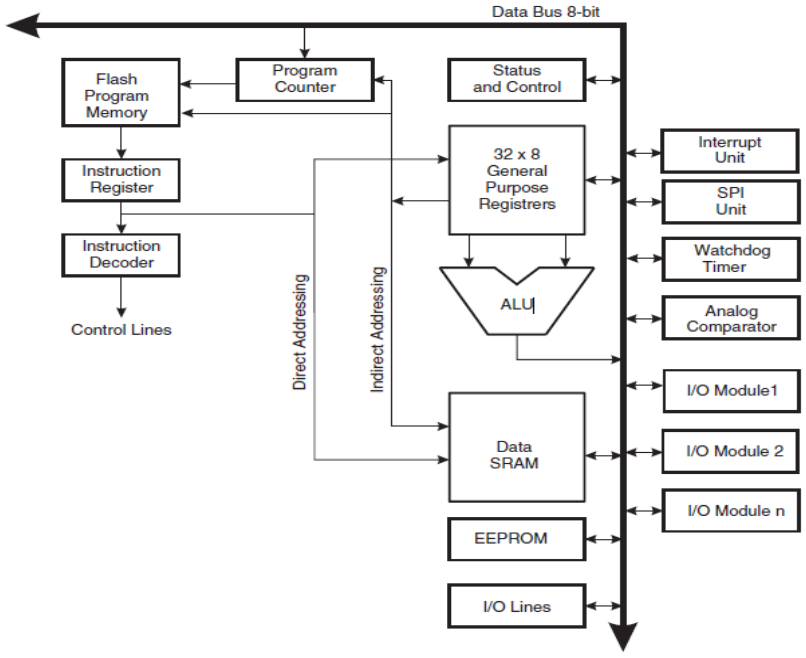

Figure 18 Block Diagram of the AVR MCU Architecture

In order to maximize performance and parallelism, the AVR uses Harvard architecture – with separate memories and buses for program and data. Instructions in the program memory are executed with a single level pipelining. While one

instruction is being executed, the next instruction is pre-fetched from the program memory. This concept enables instructions to be executed in every clock cycle. The program memory is In-System Reprogrammable Flash memory.

The fast-access Register File contains 32 × 8-bit general purpose working registers with a single clock cycle access time. This allows single-cycle Arithmetic Logic Unit (ALU) operation. In a typical ALU operation, two operands are output from the Register File, the operation is executed, and the result is stored back in the Register File – in one clock cycle.

Six of the 32 registers can be used as three 16-bit indirect address register pointers for Data Space addressing – enabling efficient address calculations. One of these address pointers can also be used as an address pointer for look up tables in Flash Program memory. These added function registers are the 16-bit X-, Y-, and Z-register.

The ALU supports arithmetic and logic operations between registers or between a constant and a register. Single register operations can also be executed in the ALU. After an arithmetic operation, the Status Register is updated to reflect information about the result of the operation.

Program flow is provided by conditional and unconditional jump and call instructions, able to directly address the whole address space. Most AVR instructions have a single 16-bit word format. Every program memory address contains a 16- or 32-bit instruction.

Program Flash memory space is divided in two sections, the Boot program section and the Application Program section. Both sections have dedicated Lock bits for write and read/write protection. The SPM instruction that writes into the Application Flash memory section must reside in the Boot Program section.

During interrupts and subroutine calls, the return address Program Counter (PC) is stored on the Stack. The Stack is effectively allocated in the general data SRAM, and consequently the Stack size is only limited by the total SRAM size and the usage of the SRAM. All user programs must initialize the SP in the reset routine (before

subroutines or interrupts are executed). The Stack Pointer SP is read/write accessible in the I/O space. The data SRAM can easily be accessed through the five different addressing modes supported in the AVR architecture.

The memory spaces in the AVR architecture are all linear and regular memory maps.

A flexible interrupt module has its control registers in the I/O space with an additional global interrupt enable bit in the Status Register. All interrupts have a separate interrupt vector in the interrupt vector table. The interrupts have priority in accordance with their interrupt vector position. The lower the interrupt vector address, the higher the priority.

The I/O memory space contains 64 addresses for CPU peripheral functions as Control Registers, SPI, and other I/O functions. The I/O Memory can be accessed directly, or as the Data Space locations following those of the Register File, $20 - $5F.

2.5.7.4 ALU – Arithmetic Logic Unit

The high-performance Atmel®AVR® ALU operates in direct connection with all the 32 general purpose working registers. Within a single clock cycle, arithmetic operations between general purpose registers or between a register and an immediate are executed. The ALU operations are divided into three main categories – arithmetic, logical, and bit-functions. Some implementations of the architecture also provide a powerful multiplier supporting both signed/unsigned multiplication and fractional format.

3 Chapter 3

Design and Development

3.1 Introduction

This chapter describes the complete procedure of the design concept and implementation process of the system. We need the current and voltage data to trace an I-V curve of a solar PV cell or module. To serve this purpose, the module is connected with a load. Different amount of load will give the different values of voltage and corresponding current. These I-V data will be used to trace an I-V curve in a PC. We will use automatic software to trace the I-V curve and calculate other parameters like fill factor, efficiency, maximum power etc. So there are two main parts of this system, firstly the hardware design, and secondly the software design where programming for the microcontroller and the parameter calculation will be implemented. The following sections and sub sections are going to describe the system with individual circuit diagram for each part with its working principle.

3.2 Hardware Design

This part of the system includes the block diagram and the individual circuit blocks with its working process. For the convenience of the reader we are going to explain each blocks of the circuit diagram. The whole system is dependable to the microcontroller (MC). So each unit is connected to the MC. complete block diagram of the system is as following

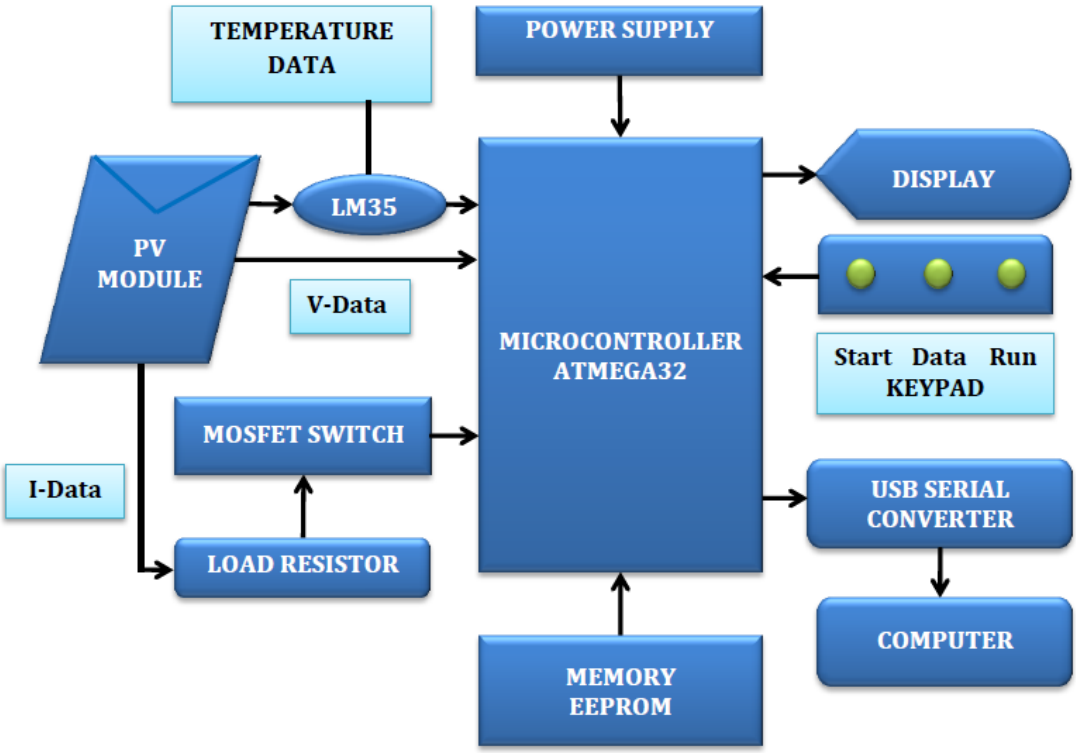

Figure 19 Block diagram of the I-V tracer

3.3 Individual Blocks of the System

The whole system is composed of eight different blocks. These blocks of the system are as following

1. System Power Supply
2. Voltage and Current Data Sensing
3. Temperature Data Sensing
4. Memory Unit
5. Display Unit
6. Keypad
7. USB Serial Converter
8. Microcontroller

Now we are going to describe these blocks below with each of their relative circuit diagrams and process of working.

3.3.1 System Power Supply

A switched-mode power supply (switching-mode power supply, switch-mode power supply, SMPS, or switcher) is an electronic power supply that incorporates a switching regulator to convert electrical power efficiently. Like other power supplies, an SMPS transfers power from a source, like mains power, to a load. Here load is the circuit of solar PV module tester, which requires regulated 5 V dc power. The power supply is the circuit that makes the 50 Hz, single phase 110-240 V ac power source converted to a 12 V DC supply.

Figure 20 Block diagram of a simple mains operated AC/DC switching mode power supply

Here we need a 5V DC supply for the microcontroller to operate it. So to ensure this, positive voltage regulator IC is a perfect component. From the switching power adapter (collected from market) positive and negative ends are connected to the terminal block. Positive terminal is connected to the rectifier diode 1N4007 and to the input of the LM7805 IC. Negative terminal is connected to the ground. One 10µF capacitor and one 104pF capacitor is used to filter the output voltage of the LM7805 IC and for smooth, noise free constant 5V supply to the microcontroller. Schematic of the power supply system is given below

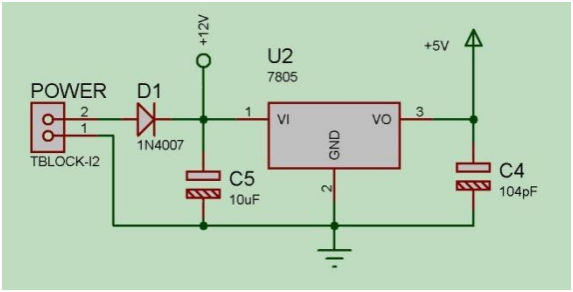

Figure 21 Schematic of the power supply system

3.3.2 Voltage and Current Data Sensing

The concept was about to reduce human effort, from manually changing the load which is connected to the solar PV module. We have used a parallel combination of three enhancement type n-channel power MOSFET (RPF70N06) to use as a switch for the system. The resistive drop ($r_{ds(on)}$) of RPF70N06 is 14mΩ. To reduce this drop we have paralleled three of them. This helps to reduce the heat generated in its operation, and thus increase overall switching efficiency, with an increase in the capability of larger watt handling of the system. There is a heat sync which holds these MOSFET's and dissipates the heat in air.

On-off mode of operation can be achieved by changing gate or base voltage from 0 to nV. Here, n is the required voltage to make the drain-source channel fully conductive. We have used Pulse Width Modulation (PWM) voltage generator for sending varying voltages to its gate. The threshold level of RPF70N06 is 10V. So minimum of 10V is required for the initialization of its required operation. But we get only 5V from the microcontroller and it is supplied as PWM. To give minimum threshold voltage we have used a photo coupler (TLP250). The PWM has given by the MC pin at port D, bit 5/OC1A to pin 2 (+LED) and pin 3 (-LED) is connected to ground. The 12V DC is connected to pin 8 (V_{cc}) of the TLP250. Output from the TLP250 is connected to the gate of the MOSFET's through a 100Ω resistance. In this way now we have 12V and 0V pulse to the gates of the MOSFET. We have used a resistor of 1Ω and 400W as the load.

We have used a simple voltage divider to sense the voltage we get from the solar PV module. To filter the output we have placed a 10µF capacitor and then connected this output to ADC pin of the microcontroller.

To sense the current we have placed a small resistance in series with the load resistor and MOSFET switch. We measure the voltage drop across this small resistance and sample this value 50 times and average this value and put it to the ADC of the microcontroller. There is a 10µF capacitor in parallel with the small resistance. When the switch is closed, this capacitor gets charged up very quickly. Now when the switch is open, this capacitor discharges very slowly through a 100kΩ resistance connected in parallel. But before it discharges the switch gets closed again. This way we get a continuous voltage signal to the ADC pin, where this value gets calculated to give the current output of the module.

Schematic of the Voltage and Current Data Sensing is given below

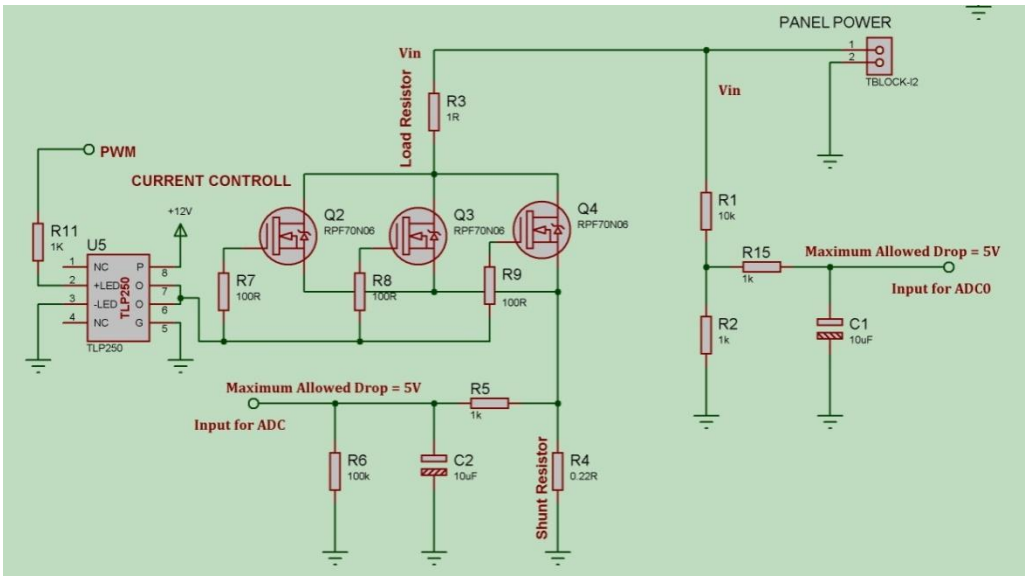

Figure 22 Schematic of the Voltage and Current Data Sensing

3.3.2.1 Measuring Voltage and Design of Voltage Divider Circuit

First of all let us discuss how do we measure voltage? Actually ATMEGA32's ADC can measure 0V to +5V, but here our voltage range is much larger than this voltage.

Hence we can't feed the input voltage directly to the controller's ADC pins. Instead of feeding directly, input voltage is reduced by a combination of voltage divider resistors.

3.3.2.2 Measuring Voltage with Atmega32 Microcontroller

Resistor R_1=10KΩ and R_2=1KΩ is used as voltage divider. According to voltage division formula, voltage less than 5 volt appear across microcontroller in the case of maximum input voltage 55 volt.

$V_{out} = (R_2 / R_1+R_2)\ xV_{in}$ (max)

$V_{out} = (1 / 10+1) \times 55 = 5$ volt

Hence at maximum input voltage of 55 volt, only 5 volt appears across microcontroller. ADC module of ATMEGA32 microcontroller converts analog signal into binary numbers. ATMEGA32 microcontroller have 10 bit ADC. So it converts analog signal to 10 bit digital number which can be back converted into voltage using following calculation in programming of digital voltmeter. Resolution is important to discuss here. Resolution means value for which ADC increment by one. For example ATMEGA32 microcontroller has 10-bit ADC and it counts binary from 0-1023 for every minimum analog value of input signal. This minimum analog value is called resolution [32].

Resolution = $(V_{ref+} - V_{ref-}) / (1024 -1)$;

In this project we are taking V_{ref+}= 5 volt and V_{ref-} = 0 volt. Hence by using these values in above formula:

Resolution = $(5 - 0)/ (1023)$ = 4.8876 mV;

It means for every analog signal of 4.88mV, ADC value increments by one. Liquid crystal display is used to display values of voltage. Maximum allowed drop will be 5V.

ATMEGA32 microcontroller's ADC reference voltage is set to V_{cc} = +5V. So what we have to do is make such a voltage divider that can divide out maximum range 55 volts to 5 volts. For this we need, Vin/11 => 55/11 = 5V voltage divider, and to keep as less as possible attenuation on the under test voltage we have to keep the voltage divider resistor value in few thousand ohms because it takes very little current from the target but as much to drive ADC of the ATMEGA32.

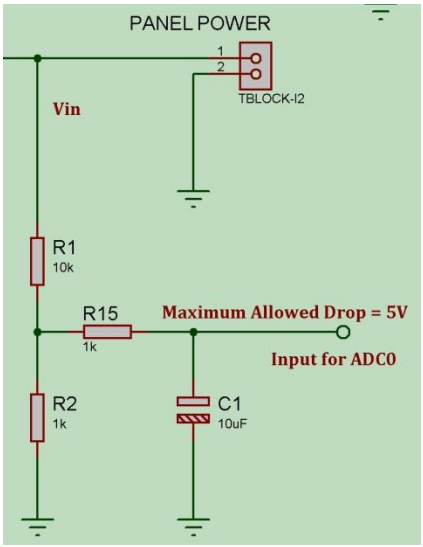

Figure 23 Schematic diagram of the voltage divider circuit

$5 = V_{in}(max) \times R_2/R_1+R_2$,

Here assume, V_{in} (max) = 55V; and R_2 = 1KΩ

$=> 5 = 55 \times 1K\Omega / R_1+R_2$

$=> R_1+R_2 = 55 \times 1K\Omega/5$

$=> R_1 = 11K\Omega - R_2$

$=> R_1 = 11K\Omega - 1K\Omega$

$=> R_1 = 10K\Omega$

Note: In case of increasing the input range, let's say 0V to 100V, change the above equations accordingly.

3.3.2.3 Calculating Actual (Real) Input Voltage from Voltage Divider Circuit

As per our circuit diagram, ATMEGA32 microcontroller reads voltage across 1KΩ resistor. So calculating voltage across 1KΩ resistor by voltage divider rule:

Assume V1 is the voltage across 1KΩ resistor

$V_1 = (V_{in} / 10K\Omega + 1K\Omega) \times 1K\Omega$

$\Rightarrow V_1 = (V_{in} / 11K\Omega) \times 1K\Omega$

This V_1 is read by the ATMEGA32 microcontroller's ADC module. Hence the actual input is

$V_{in} = (V_1 \times 11K\Omega) / 1K\Omega$

$\Rightarrow V_{in} = V_1 \times 11K\Omega$

3.3.2.4 Mapping ADC Values to Input Voltage

ATMEGA32 microcontroller's ADC is a 10 bit ADC, which means the output of ADC can be vary from0 to 1023 maximum while input varies from 0 to 5V.That is when the input voltage is +5V then ADC value is 1023, when input voltage is 0V ADC value will be 0.We have to map $0 \rightarrow 1023$ to $0 \rightarrow 5$; it can be done by multiplying ADC value with 1000 to make it an integer and then dividing this value with a constant K.

K = (Maximum ADC Voltage) / (Maximum ADC Value)

$\Rightarrow K = 5 / 1023$

$\Rightarrow K = 0.0048876$

=> K = 4.88mV

Now as stated above, 10 bit ADC resolution we get is 1023 maximum count with 5V reference. So we get 5/1023 = 0.0048878 V/Count. Now if we apply the voltage divider rule then we get 12 x (1/11) = 1.09090V = 1.09090 x 1000 = 1090.9mV, now to get the count we have to divide this value with K = 4.88mV, hence we get 1090.9/4.88 = 223.54508 count, that means if the ADC count is 223.54508 then input voltage is 223.54508 x 4.88 = 1090.9mV. But with the voltage divider the maximum voltage is 55V, so the calculations will be 55/1023= 0.05376 volts/count, so for 223.54508 count we get 223.54508 x 0.05376 = 12.0 Volts.

Hence, V_{actual} = (ADC Value x 4.8878 x 11) = 12 Volts

3.3.2.5 Current Sensing Circuit Using ATMEGA32 Microcontroller

Schematic diagram of current sensing circuit using ATMEGA32 microcontroller is given below. In this circuit diagram Maximum 55 volt dc source is applied to 1Ω load. Current passing through this load is measured with the help of shunt resistor and ATMEGA32 microcontroller. Now the question is why we need shunt resistor to measure current?

3.3.2.6 Need of Shunt Resistor

Microcontrollers or any microcomputer system cannot read current directly. Microcontrollers only sense voltage. Microcontroller's logic high and low is also based on voltage level. Therefore microcontrollers do not sense current directly. That is why we need to sense current into voltage form. Shunt resistor is used to convert current into voltage form. When current passes through shunt resistor, voltage appears across shunt resistor. This voltage can be easily measured with the help of analog to digital converter channel of ATMEGA32 microcontroller. This measured voltage value can be converted back into current in programming using ohm's law formula:

V = IR;

Shunt resistor value is known and voltage is measured with microcontroller. So current can be easily calculated by using above Ohm's law formula.

I = V/R

In ATMEGA32, we are going use 10bit ADC (Analog to Digital Conversion) feature to do this. Although we have few other ways to get the current parameter from a circuit, we are going to use resistive drop method, because it's the easiest and simplest way to get current parameter.

In this circuit 0.22 ohm 20W shunt resistor is used. Now you must be wondering how to design this low resistance value resistor? The simplest solution to this problem is to take a piece of wire and makes it few turn. After making few turns, measure its resistance with the help of ohm meter. It is easy to design 0.22 Ω resistors with the help of simple wire. It is a hit and trail method. Keep trying until successfully get a value close to .22 ohm. Other option is to use Hall Effect current sensor which converts current into voltage directly. Magnitude of voltage depends on magnitude of current. Here we have used a 0.22Ω 20W resistor collected from market.

1K ohm resistor at the input of analog to digital converter is used to protect microcontroller from high current, because current always follow a low resistance path. If we don't use any resistance there, current will start to flow towards microcontroller instead of shunt resistor. It will damage microcontroller permanently, because voltage more than 5 volt may damage microcontroller permanently. LCD is interfaced with ATMEGA32 microcontroller to display current value.

In this method we are going to pass the current which needed to be measured in to a small resistance, by this we get a drop across that resistance which is related to current flowing through it. This voltage across resistance is fed to ATMEGA32 for ADC conversion. With that we will have the current in digital value which will be displayed on a 16x2 LCD. When current changes there will be drop change in the

resistance which is linear to it. So with this we have a voltage which changes with linearity.

Now important thing to note here is, the input taken by the controller for ADC conversion is as low as 50µAmp. This loading effect of resistance based voltage divider is important as the current drawn from V_{out} of voltage divider increases the error percentage. But we can ignore this for now.

3.3.2.7 Circuit Diagram and Working Explanation

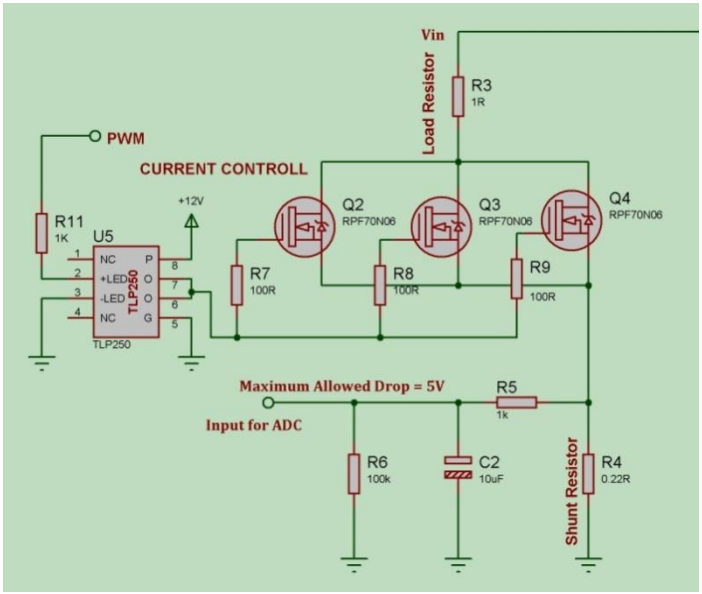

Figure 24 Schematic diagram of the current sensing of the system

In ATMEGA32 microcontroller, the ADC is of 10 bit resolution, so the controller can detect a minimum change of $V_{ref}/2^{10}$, so if the reference voltage is 5V we get a digital output increment for every $5/2^{10}$ = 4.88mV. So for every 4.88mV increment in the input we will have an increment of one at digital output.

Now we need to set the register of ADC based on the following terms:

1. First of all we need to enable the ADC feature in ADC.

2. Here we are going to get a maximum input voltage for ADC conversion is +5V. So we can set up maximum value or reference of ADC to 5V.

3. The controller has a trigger conversion feature that means ADC conversion takes place only after an external trigger, since we don't want that we need to set the registers for the ADC to run in continuous free running mode.

4. For any ADC, frequency of conversion (Analog value to Digital value) and accuracy of digital output are inversely proportional. So for better accuracy of digital output we have to choose lesser frequency. For normal ADC clock we are setting the presale of ADC to maximum value (2). Since we are using the internal clock of 1MHZ, the clock of ADC will be (1000000/2).

These are the only four things we need to know to getting started with ADC.

All the above four features are set by two registers,

ADC Multiplexer Selection Register – ADMUX

Bit	7	6	5	4	3	2	1	0	
	REFS1	REFS0	ADLAR	MUX4	MUX3	MUX2	MUX1	MUX0	ADMUX
Read/Write	R/W	R/W	R/W	R/W	R/W	R/W	R/W	R/W	
Initial Value	0	0	0	0	0	0	0	0	

ADC Control and Status Register A – ADCSRA

Bit	7	6	5	4	3	2	1	0	
	ADEN	ADSC	ADATE	ADIF	ADIE	ADPS2	ADPS1	ADPS0	ADCSRA
Read/Write	R/W	R/W	R/W	R/W	R/W	R/W	R/W	R/W	
Initial Value	0	0	0	0	0	0	0	0	

RED (ADEN): This bit has to be set for enabling the ADC feature of ATMEGA.

BLUE (REFS1,REFS 0): These two bits are used to set the reference voltage (or max input voltage we are going to give). Since we want to have reference voltage 5V, REFS0 should be set, by the table.

REFS1	REFS0	Voltage Reference Selection
0	0	AREF, Internal Vref turned off
0	1	AVCC with external capacitor at AREF pin
1	0	Reserved
1	1	Internal 2.56V Voltage Reference with external capacitor at AREF pin

YELLOW (ADFR): This bit must be set for the ADC to run continuously (free running mode).

PINK (MUX0-MUX3): These four bits are for telling the input channel. Since we are going to use ADC0 or PIN0, we need not set any bits as by the table.

MUX3..0	Single Ended Input
0000	ADC0
0001	ADC1
0010	ADC2
0011	ADC3
0100	ADC4
0101	ADC5
0110	ADC6
0111	ADC7
1000	
1001	
1010	
1011	

BROWN (ADPS0-ADPS2): these three bits are for setting the prescalar for ADC. Since we are using a prescalar of 2, we have to set one bit.

ADPS2	ADPS1	ADPS0	Division Factor
0	0	0	2
0	0	1	2
0	1	0	4
0	1	1	8
1	0	0	16
1	0	1	32
1	1	0	64
1	1	1	128

DARK GREEN (ADSC): this bit set for the ADC to start conversion. This bit can be disabled in the program when we need to stop the conversion.

3.3.3 Temperature Data Sensing

We have used LM35 temperature sensor to sense the temperature of the module when testing operation was conducted. For 1°C increase in temperature there is an increase of 10mV. Its V_{cc} is connected with +5Vdc and V_{ss} is connected to GND of the circuit. The output is connected to the ADC pin of the microcontroller. There is a 1µF capacitor in parallel with V_{out} pin of the sensor to filter the output before give it as the input for the ADC of the microcontroller. Schematic of temperature data sensing is given below

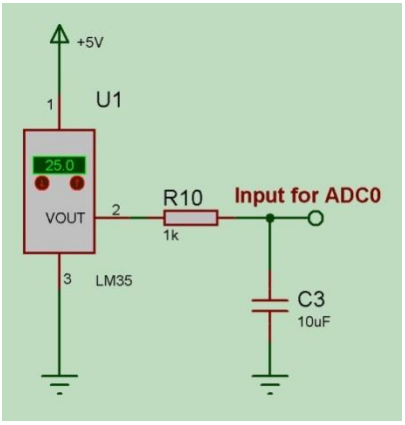

Figure 25 Schematic of temperature data sensing

3.3.4 Memory Unit

In this block of the circuit we have used an electrically erasable and programmable read only memory EEPROM (AT24C512B) for storage of our measured data. The

communication of this IC with the microcontroller has completed by the inter integrated circuit (I^2C).

The I2C-bus supports any IC fabrication process (NMOS, CMOS, bipolar). Two wires, serial data (SDA) and serial clock (SCL), carry information between the devices connected to the bus. Each device is recognised by a unique address- whether it's a microcontroller, LCD driver, and memory or keyboard interface- and can operate as either a transmitter or receiver, depending on the function of the device. Obviously an LCD driver is only a receiver, whereas a memory can both receive and transmit data. In addition to transmitters and receivers, devices can also be considered as masters or slaves when performing data transfers (see Table 2). A master is the device which initiates a data transfer on the bus and generates the clock signals to permit that transfer. At that time, any device addressed is considered a slave.

3.3.4.1 Definition of I2C-bus terminology

TERM	**DESCRIPTION**
Transmitter	The device which sends the data to the bus
Receiver	The device which receives the data from the bus
Master	The device which initiates a transfer, generates clock signals and terminates a transfer
Slave	The device addressed by a master
Multi-master	More than one master can attempt to control the bus at the same time without corrupting the message
Arbitration	Procedure to ensure that, if more than one master simultaneously tries to control the bus, only one is allowed to do, so and the message is not corrupted
Synchronization	Procedure to synchronize the clock signals of two or more devices

Table 2 Definition of I2C-bus terminology

The I2C-bus is a multi-master bus. This means that more than one device capable of controlling the bus can be connected to it. As masters are usually micro-controllers, let's consider the case of a data transfer between two microcontrollers connected to the I2C-bus. This highlights the master-slave and receiver-transmitter relationships to be found on the I2C-bus. It should be noted that these relationships are not permanent, but only depend on the direction of data transfer at that time. The transfer of data would proceed as follows:

1. Suppose microcontroller A wants to send information to microcontroller B:

- Microcontroller A (master), addresses microcontroller B (slave)
- Microcontroller A (master-transmitter), sends data to microcontroller B (slave-receiver)
- Microcontroller A terminates the transfer.

2. If microcontroller A wants to receive information from microcontroller B:

- Microcontroller A (master) addresses microcontroller B (slave)
- Microcontroller A (master-receiver) receives data from microcontroller B (slave-transmitter)
- Microcontroller A terminates the transfer.

Even in this case, the master (microcontroller A) generates the timing and terminates the transfer.

The possibility of connecting more than one microcontroller to the I2C-bus means that more than one master could try to initiate a data transfer at the same time. To avoid the chaos that might ensue from such an event — an arbitration procedure has been developed. This procedure relies on the wired-AND connection of all I2C interfaces to the I2C-bus.

If two or more masters try to put information onto the bus, the first to produce a 'one' when the other produces a 'zero' will lose the arbitration. The clock signals during arbitration are a synchronized combination of the clocks generated by the masters using the wired-AND connection to the SCL line.

Generation of clock signals on the I2C-bus is always the responsibility of master devices; each master generates its own clock signals when transferring data on the bus. Bus clock signals from a master can only be altered when they are stretched by a slow-slave device holding-down the clock line or by another master when arbitration occurs.

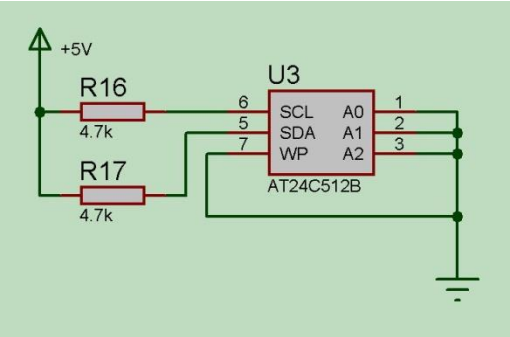

Figure 26 Schematic diagram of the EEPROM

3.3.5 Display

LCD (Liquid Crystal Display) screen is an electronic display module and find a wide range of applications. A 16x2 LCD display is very basic module and is very commonly used in various devices and circuits. These modules are preferred over seven segments and other multi segment LEDs.

A 16x2 LCD means it can display 16 characters per line and there are 2 such lines. In this LCD each character is displayed in 5x7 pixel matrix. This LCD has two registers, namely, Command and Data. The command register stores the command instructions given to the LCD. A command is an instruction given to LCD to do a predefined task like initializing it, clearing its screen, setting the cursor position, controlling display etc. The data register stores the data to be displayed on the LCD. The data is the ASCII value of the character to be displayed on the LCD.

Liquid Crystal Display (LCD) is very helpful in providing user interface as well as for debugging purpose. The most common type of LCD controller is HITACHI 44780 which provides a simple interface between the controller & an LCD.

A 16x2 LCD consist of 16 pin that make connections to display a text on it. It can be interfaced with any controller to control the displayed images on it.

Pin No:	Name	Function	Pin No:	Name	Function
1	VSS	This pin must be connected to the ground	9	DB2	Data
2	VCC	Positive supply voltage pin (5V DC)	10	DB3	Data
3	VEE	Contrast adjustment	11	DB4	Data
4	RS	Register selection	12	DB5	Data
5	R/W	Read or write	13	DB6	Data
6	E	Enable	14	DB7	Data
7	DB0	Data	15	LED+	Back light LED+
8	DB1	Data	16	LED-	Back light LED-

Table 3 Pin description of the 16 character 2 line LCD

3.3.5.1 Interfacing with LCD

The LCD requires 3 control lines (RS, R/W & EN) & 8 or 4 data lines. The number on data lines depends on the mode of operation. If operated in 8-bit mode then 8 data lines + 3 control lines i.e. total 11 lines are required. And if operated in 4-bit mode then 4 data lines + 3 control lines i.e. 7 lines are required. Here we used 4-bit mode.

When **RS is low (0),** the data is to be treated as a command. When RS is high (1), the data being sent is considered as text data which should be displayed on the screen. This pin is connected to the MC at Port B, Bit 7/SCK. When **R/W is low (0),** the information on the data bus is being written to the LCD. When RW is high (1), the program is effectively reading from the LCD. In our system there is no need to read from the LCD so this line is directly connected to Ground thus saving one controller line. The **ENABLE pin** is used to latch the data present on the data pins. A HIGH - LOW signal is required to latch the data. The LCD interprets and executes our command at the instant the EN line is brought low. If you never bring EN low, your

instruction will never be executed. This pin is connected to the MC at port b, bit 6/ MISO. Data pin D7-D4 is connected to the MC in port B, bit 2 to port b, bit 5. V_{CC} is connected to 5V power supply which is pin 2 and pin 1 & 3 is connected to ground. Schematic of the Display Block is as following

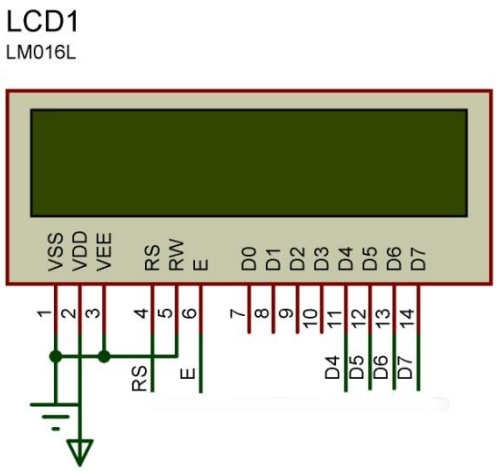

Figure 27 Schematic of the Liquid Crystal Display Unit

3.3.6 Keypad

The system we made contains a combination of three button switches whose ends are connected to ground and the other three ends are connected to three ADC pins through three resistances of 10kΩ each. These ADC pins are internally pulled up, that means there are 5 volts in each pin. Now when we press a button switch or we close the path to ground, the pin gets pulled down. Like this way we complete the test or the system responds to our commands. The schematic of the keypad is presented below.

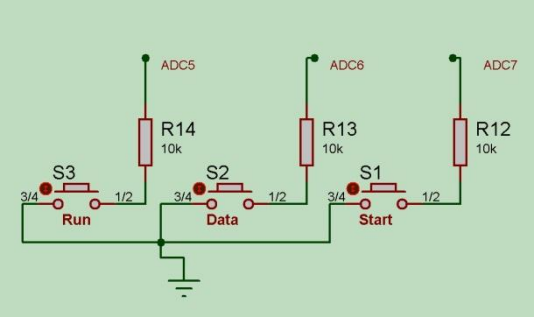

Figure 28 Schematic diagram presenting keypad of the system

3.3.7 USB Serial Converter

The USB-TTL Interface Module (for brevity, Module hereafter) can be used to add USB connectivity to any microcontroller or other device that is capable of standard serial communication. There are several configuration options on the Module that facilitate its use in a variety of situations. The Module can be powered from the USB hub or from an external supply. When powered by the USB hub, the Module can optionally provide power to external circuitry. The Module can be configured for either a 5 volt or a 3.3 volt signal interface and it can provide 3.3 volt power to external circuitry as well, subject to current limits.

The pin out of the Module is designed to make it very easy to use with a microcontroller that uses the standard Basic Stamp pin out. Transmit and receive data pin, DTR and ground connections are in the correct order so that the Module can be directly connected to a compatible microcontroller on a solder less breadboard. Schematic of the USB serial converter is given below

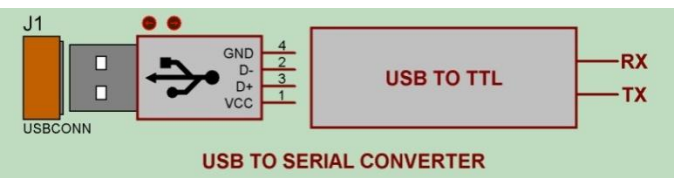

Figure 29 Schematic diagram of the USB serial converter

This USB to TTL module use a FT232 device to communicate with the RX and TX pin of the microcontroller. This is called serial communication. The FT232R is a USB to serial UART (universal asynchronous receiver/transmitter) interface with optional clock generator output. In addition, asynchronous and synchronous bit bang interface modes are available. USB to serial designs using the FT232R have been further simplified by fully integrating the external EEPROM, clock circuit and USB resistors onto the device. A UART is usually an individual (or part of an) integrated circuit (IC) used for serial communications over a computer or peripheral device serial port. UARTs are now commonly included in microcontrollers. The universal asynchronous receiver/transmitter (UART) takes bytes of data and transmits the individual bits in a sequential fashion. At the destination, a second UART re-assembles the bits into complete bytes. Each UART contains a shift register, which is the fundamental method of conversion between serial and parallel forms. Serial transmission of digital information (bits) through a single wire or other medium is less costly than parallel transmission through multiple wires. Now to interface with a computer FTDI driver is a must. We have installed the driver to get the USB to TTL module interfaced with the computer. The driver was downloaded from the website of the FTDI Chip limited and it is a free to use driver.

3.3.8 Microcontroller

Finally all of the individual blocks made their connections with the microcontroller IC. This microcontroller IC controls all other blocks in our system. Microcontroller needs constant +5V power supply to operate. So we have made a constant +5V power supply using positive voltage regulator IC LM7805. This microcontroller has the operating frequency of 8MHz. ATMEGA32 includes two timer counter of 8bit and 16 bit. In our system design we have programmed for the 10bit timer. So we got 8MHz/1023 = 7.82 KHz of frequency for the operation, which have proved enough for the accuracy of the system. For the input of the current, voltage and temperature data we have used the analog to digital ports which includes 10bit conversion

process. In this way if we calculate for the minimum voltage require to sense as 1bit count we get 5000/1023 = 4.8876mV. Here 5000mV stands for the +5V, which is the reference voltage of the system. After taking the input ADC converts these analog data to digital bit count and we convert this again to get the desired current, voltage and temperature data. In the poragramming of the microcontroller part we have calibrated the current, voltage and temperature data to get the actual reading from the system.

Voltage calibration

To calibrate the voltage data we get from the ADC we have measured the panel input voltage from the input terminal with a digital multimeter. Now we took the reading from the LCD of voltage and from this we got the ratio to be calibrated for getting the actual voltage data. In the programme we multiplied this ratio with the ADC output and there we have our actual voltage displaying on the LCD.

Current Calibration

In this portion of the system we are taking the voltage drop occurs through a fixed low resistance value which is called the shunt resistance. Now we measure the drop when the resistance gets a pulse from the microcontroller with the MOSFET switch is closed. We increase this pulse at 1023 steps and for each step we measure the drop 50 times and divide by 50 to get the accurate voltage data. Now we through the ADC we get the bit count of this voltage data. From these values we calculate the current with Ohm's Law. Now to calibrate this current data at first we short the panel and measure the current from the input terminal of the system. Taking the output from the LCD we calculate the conversion ratio of the current. Now in the programme we multiply this ratio with the ADC value to get the actual current dat.

Temperature Calibration

LM35 temperature sensor increases 1°C of temperature for the increase of 10mV. We have 4.88mV sensing voltage for each bit. So to get the actual reading we have divided the ADC value with 2 which gives us the actual temperature data.

For the keypad instruction we have used the ADC ports which are in normal pulled up internally. So we designed the keypad to pull down these pins to complete the instructions given by the operator. For data transmitting and receiving to and from a computer we have used the TX, RX pins or port D. Pulse width modulation has also given from port D. For storing the I-V-T data we have used an EEPROM and to complete data TX, RX I^2C bus communication has been employed. Port C of the microcontroller has used for the data storing in the EEPROM of the system.The result of the system has displayed in a LCD, which has been connected to the port B of the microcontroller. Complete schematic diagram of the system is as following

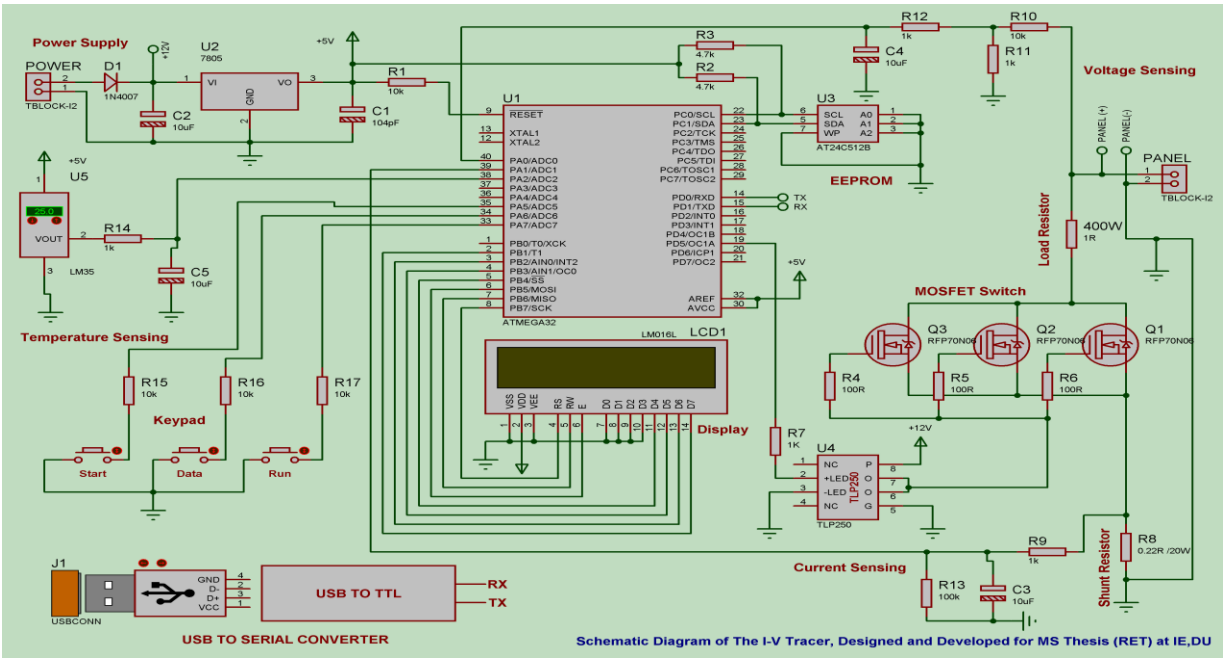

Figure 30 Schematic diagram of the I-V tracer

3.4 Simulation Tool for Circuit

We have used circuit simulation software tool for our system before we started implementing our system hardware practically. The tool we have used is Proteus Virtual System Modeling (VSM). In the following sections and sub section we are

going to introduce you with the Proteus and PCB design using this software tool with the simulating circuit diagram of the system we have designed.

3.4.1 Proteus VSM

Proteus Virtual System Modeling (VSM) combines mixed mode SPICE circuit simulation, animated components and microprocessor models to facilitate co-simulation of complete microcontroller based designs. For the first time ever, it is possible to develop and test such designs before a physical prototype is constructed.

This is possible because one can interact with the design using on screen indicators such as LED and LCD displays and actuators such as switches and buttons. The simulation takes place in real time (or near enough to it): a 1GMHz Pentium III can simulate a basic 8051 system clocking at over 12MHz. Proteus VSM also provides extensive debugging facilities including breakpoints, single stepping and variable display for both assembly code and high level language source.

3.4.2 Circuit Simulation

At the heart of Proteus VSM is ProSPICE. This is an established product that combines uses a SPICE3f5 analogue simulator kernel with a fast event-driven digital simulator to provide seamless mixed-mode simulation. The use of a SPICE kernel lets you utilise any of the numerous manufacturer-supplied SPICE models now available and around 6000 of these are included with the package.

Proteus VSM includes a number of virtual instruments including an Oscilloscope, Logic Analyser, Function Generator, Pattern Generator, Counter Timer and Virtual Terminal as well as simple voltmeters and ammeters. In addition,

we provide dedicated Master/Slave/Monitor mode protocol analysers for SPI and I2C - simply wire them onto the serial lines and monitor or interact with the data live during simulation. This tool gives a truly invaluable (and inexpensive!) way to get your communication software right prior to hardware prototyping.

Should you wish to take detailed measurements on graphs, or perform other analysis types such as frequency, distortion, noise or sweep analyses of analogue circuits, you can purchase the Advanced Simulation Option. This option also includes Conformance Analysis - a unique and powerful tool for Software Quality Assurance.

3.4.3 Co-Simulation of Microcontroller Software

The most exciting and important feature of Proteus VSM is its ability to simulate the interaction between software running on a microcontroller and any analog or digital electronics connected to it.

The micro-controller model sits on the schematic along with the other elements of your product design. It simulates the execution of your object code (machine code), just like a real chip. If the program code writes to a port, the logic levels in circuit change accordingly, and if the circuit changes the state of the processor's pins, this will be seen by your program code, just as in real life.

The VSM CPU models fully simulate I/O ports, interrupts, timers, USARTs and all other peripherals present on each supported processor. It is anything but a simple software simulator since the interaction of all these peripherals with the external circuit is fully modeled down to waveform level and the entire system is therefore simulated.

VSM can even simulate designs containing multiple CPUs, since it is a simple enough matter to place two or more processors on a schematic and wire them together [33].

3.4.4 PCB Design

A PCB is a printed circuit board, also known as a printed wiring board. It is used in electronics to build electronic devices. A PCB serves two purposes in the construction of an electronic device; it is a place to mount the components and it provides the means of electrical connection between the components.

A PCB starts out as a thin, non-conducting sheet of material. The most common material used is a glass fiber epoxy laminate material. A thin layer of copper is then chemically deposited on each side of this material.

The next step is to "print" the connection diagram onto the PCB. The connection diagram is the wiring required to connect the components. In the very early days of electronics, these connections were in fact done with wires. This is the reason PCBs are also sometimes referred to as printed wiring boards. The "printing" is usually done by photographically transferring the image to the board. This image is "printed" with an acid resistant material.

Next, the PCB is put into an acid bath. The acid bath removes the copper from the board, excepting the areas protected by the resistant material. This process leaves the connections or wiring "printed" on the PCB. Next, holes are drilled in the board to allow the components to be mounted to the board and the PCB itself to be mounted to the case protecting the electronics. Finally, a protective coating is applied to the board to prevent corrosion of the copper traces. From various types of PCB design software it is better to use Proteus VSM and PCB design tool.

Proteus PCB design combines the schematic capture and ARES PCB layout programs to provide a powerful, integrated and easy to use suite of tools for professional PCB Design.

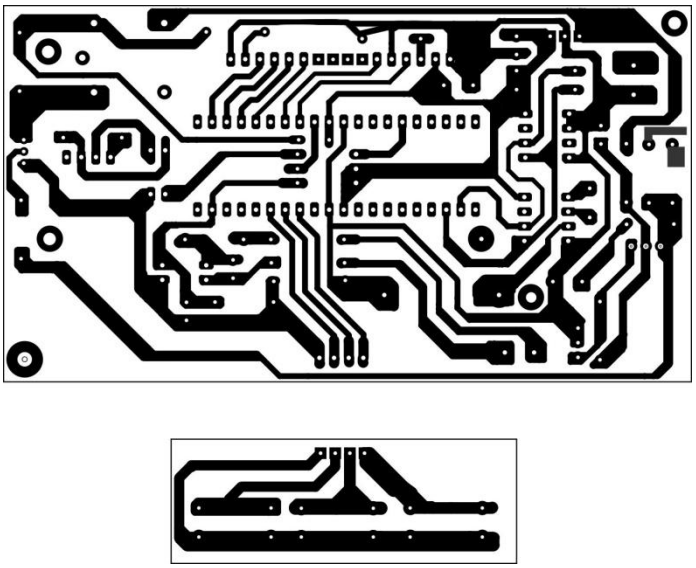

Figure 31 PCB of the I-V tracer circuit

All Proteus PCB design products include an integrated shape based auto router and a basic SPICE simulation capability as standard. More advanced routing modes are included in Proteus PCB Design Level 2 and higher whilst simulation capabilities can be enhanced by purchasing the Advanced Simulation option and/or micro-controller simulation capabilities.

3.5 Software Design

There are two parts of this section of the design. One is the programming section for the microcontroller of the hardware system. The other part is the software section, which explains the data manipulation, collected from the microcontroller and displays the results of the analyzed I-V data.

For microcontroller programming we have used the C programming language and the CodeVisionAVR compiler. The analyzing part has completed with the Java Programming language and Java Development Kit with Java SE 8 developing software. Brief introduction of the tools are given in the following sub sections.

3.5.1 Programming of the Microcontroller

The system we have presented in this paper is designed and developed based on microcontroller IC. For microcontroller there are many language and compiler around the world. We have used "C++" as our programming language of the microcontroller. CodeVisionAVR is a C cross-compiler and we have used this compiler for our program. There are no needs of any other software tools to convert the programme written in C to .hex file. CodeVisionAVR made this easy for the code writers as one have to write only the programme in C and the rest will do this tool. Brief introduction of C programming language and CodeVisionAVR are given below.

3.5.2 C Programming Language

C is one of the most widely used programming languages of all time, and there are very few computer architectures for which a C compiler does not exist. C is an imperative (procedural) language. It was designed to be compiled using a relatively straightforward compiler, to provide low-level access to memory, to provide language constructs that map efficiently to machine instructions, and to require minimal run-time support. C was therefore useful for many applications that had formerly been coded in assembly language, such as in system programming.

Despite its low-level capabilities, the language was designed to encourage cross-platform programming. A standards-compliant and portably written C program can be compiled for a very wide variety of computer platforms and operating systems with few changes to its source code. The language has become available on a very wide range of platforms, from embedded microcontrollers to supercomputers [34].

Advantages of C Language

- There are a small, fixed number of keywords, including a full set of flow of control primitives: for, if/else, while, switch, and do/while.
- There are a large number of arithmetical and logical operators, such as +, +=, ++, &, ~, etc
- More than one assignment may be performed in a single statement.
- Function return values can be ignored when not needed.
- User-defined (typedef) and compound types are possible.
- Low-level access to computer memory is possible by converting machine addresses to typed pointers.
- Functions may not be defined within the lexical scope of other functions.
- Function and data pointers permit *ad hoc* run-time polymorphism.
- Complex functionality such as I/O, string manipulation, and mathematical functions are consistently delegated to library routines. C does not include some features found in newer, more modern high-level languages, including object orientation and garbage collection.

3.5.3 CodeVisionAVR Compiler for Programme

CodeVisionAVR is a C cross-compiler, Integrated Development Environment and Automatic Program Generator designed for the Atmel AVR family of microcontrollers.

It is designed to run under the Windows XP, Vista, 7, 8 and 10, 32bit and 64bit operating systems.

The C cross-compiler implements all the elements of the ANSI C language, as allowed by the AVR architecture, with some features added to take advantage of specificity of the AVR architecture and the embedded system needs.

The compiled COFF object files can be C source level debugged, with variable watching, using the Atmel Studio and AVR Studio debuggers.

The Integrated Development Environment (IDE) has built-in AVR Chip In-System Programmer software that enables the automatic transfer of the program to the microcontroller chip after successful compilation/assembly. The In-System Programmer software is designed to work in conjunction with the Atmel STK500, STK600, AVRISP, AVRISP MkII, AVR Dragon, JTAGICE MkII, JTAGICE 3,Atmel-ICE, AVRProg (AVR9IO application note), Kanda Systems STK200+, STK300, Arduino, Dontronics DTOO6, Vogel Elektronik VTEC-ISP, Futurlec JRAVR and MicroTronics' ATCPU,Mega2000 development boards.

For debugging embedded systems, which employ serial communication, the IDE has a built-in Terminal.

CodeVisionAVR can be also used as an extension in Atmel Studio 6.2 or 7.0, allowing seamless editing, compiling and debugging projects in this IDE.

Besides the standard C libraries, the CodeVisionAVR C compiler has dedicated libraries for:

- Alphanumeric and Graphic LCD/OLED displays
- Philips 12C bus
- Texas Instruments LM75 Temperature Sensor
- Philips PCF8563, PCF8583, Maxim D51302, DS1307, DS3231 Real Time Clocks
- Maxim/Dallas Semiconductor 1 Wire protocol
- Maxim DS1820, DS18S2O and DS18B2O Temperature Sensors
- Maxim DS1621 Thermometer/Thermostat
- Maxim DS2430 and D52433 EEPROMs
- SPI
- TWI for both XMEGA and non-XMEGA chips
- USB for both XMEGA and non-XMEGA chips
- Power management

- Delays
- Gray code conversion
- MMC/SD/SD HO FLASH memory cards low level access
- FAT access on MMC/SD/SD HO FLASH memory cards
- ADS7843 and ADS7846 Resistive touchscreen controllers
- FT5206, FT5306 and FT5406 Capacitive touchscreen controllers
- BMPO85, BMP1 80 and MS561 1-01 BA Digital Pressure sensors.

CodeVisionAVR also contains the CodeWizardAVR Automatic Program Generator that allows one to write, in a matter of minutes, all the code needed for implementing the following functions:

- External memory access setup
- Chip reset source identification
- Input/output Port initialization
- External Interrupts initialization
- Timers/Counters initialization
- Watchdog Timer initialization
- UART (USART) initialization and interrupt driven buffered serial communication
- Analog Comparator initialization
- ADC and DAC initialization
- SPI Interface initialization
- Two Wire Interface initialization
- USB Initialization
- CAN Interface initialization
- 1^2C Bus, LM75 Temperature Sensor, D51621 Thermometer/Thermostat and PCF8563, PCF8583,DS1302, DS1307, DS3231 Real Time Clocks initialization
- 1 Wire Bus and DS1820/DS18S2O Temperature Sensors initialization
- Alphanumeric and graphic displays initialization
- Touchscreen controller's initialization.

CodeVisionAVR is © Copyright 1998-2015 Pavel Haiduc and HP InfoTech S.R.L., all rights reserved. The MMC, SD, SD HC and FAT File System libraries are based on the FatFS open source project from http://elm-chan.orçj © Copyright 2006-2009 ChaN, all rights reserved.

The CodeVisionAVR IDE uses the freeware TDiff Delphi component © 2001-2008 by Angus Johnson [35].

3.5.4 Flow Diagram of the Programme

In this sub section we are going to describe briefly the operation sequence of the hardware system we have designed and implemented with a program flow diagram. First of all, declarations of variables have done. As the system is connected to mains, system initialization completed with the initialize of PWM, PORT, ADC, LCD, I^2C, RX and TX. Now the status of the system displayed in the LCD. To start the I-V test we need to press the run switch and PWM starts as displaying percentage done. After completion of test, data command will display the voltage and current at maximum power. The tested I-V data will be sent to a pc through a USB data cable after the run command. If we want to interrupt the process we have to press start or run switch and this will take us back to the system ready status.

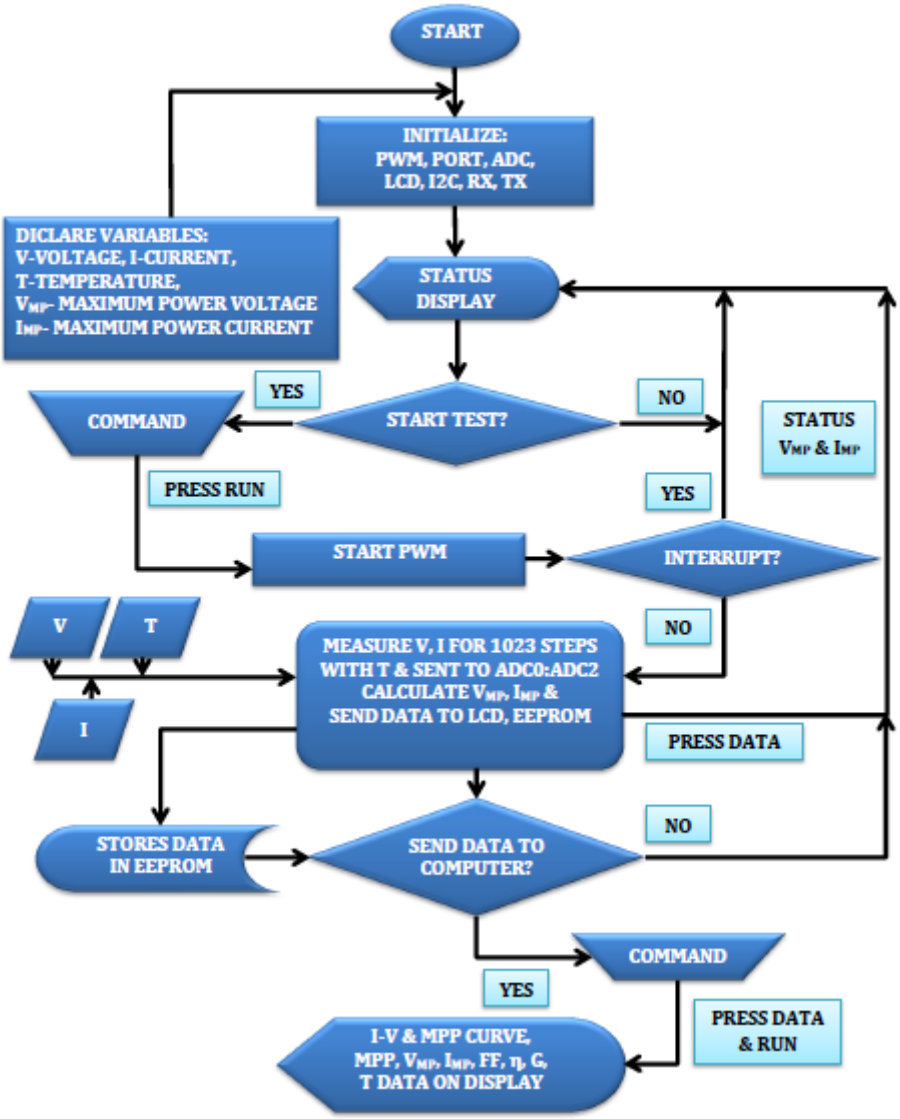

Figure 32 Flow diagram of the microcontroller program in our system

3.5.5 Java Programming Language

The Java® programming language is a general-purpose, concurrent, class based, object-oriented language. It is designed to be simple enough that many programmers can achieve fluency in the language. The Java programming language is related to C and C++ but is organized rather differently, with a number of aspects of C and C++ omitted and a few ideas from other languages included. It is intended to

be a production language, not a research language, and so, as C. A. R. Hoare suggested in his classic paper on language design, the design has avoided including new and untested features.

The Java programming language is strongly and statically typed. This specification clearly distinguishes between the compile-time errors that can and must be detected at compile time, and those that occur at run time. Compile time normally consists of translating programs into a machine-independent byte code representation. Run-time activities include loading and linking of the classes needed to execute a program, optional machine code generation and dynamic optimization of the program, and actual program execution.

The Java programming language is a relatively high-level language, in that details of the machine representation are not available through the language. It includes automatic storage management, typically using a garbage collector, to avoid the safety problems of explicit deallocation (as in C's free or C++'s delete).High-performance garbage-collected implementations can have bounded pauses to support systems programming and real-time applications. The language does not include any unsafe constructs, such as array accesses without index checking, since such unsafe constructs would cause a program to behave in an unspecified way.

The Java programming language is normally compiled to the bytecode instruction set and binary format defined in The Java Virtual Machine Specification, Java SE 8 Edition.

3.5.6 Java Platform

The Java platform is a suite of programs that facilitate developing and running programs written in the Java programming language. The platform is not specific to any one processor or operating system, rather an execution engine (called a virtual machine) and a compiler with a set of libraries are implemented for various

hardware and operating systems so that Java programs can run identically on all of them. There are multiple platforms, each targeting a different class of devices:

Java Card: A technology that allows small Java-based applications (applets) to be run securely on smart cards and similar small-memory devices.

Java ME (Micro Edition): Specifies several different sets of libraries (known as profiles) for devices with limited storage, display, and power capacities, Often used to develop applications for mobile devices, PDAs, TV set-top boxes, and printers.

Java SE (Standard Edition): For general-purpose use on desktop PCs, servers and similar devices.

Java EE (Enterprise Edition): Java SE plus various APIs useful for multi-tier client–server enterprise applications.

The Java platform consists of several programs, each of which provides a portion of its overall capabilities. For example, the Java compiler which converts Java source code into Java bytecode (an intermediate language for the JVM), is provided as part of the Java Development Kit (JDK). The Java Runtime Environment (JRE), complementing the JVM with a just-in-time (JIT) compiler, converts intermediate bytecode into native machine code on the fly. An extensive set of libraries are also part of the Java platform.

The essential components in the platform are the Java language compiler, the libraries, and the runtime environment in which Java intermediate bytecode executes according to the rules laid out in the virtual machine specification.

3.5.7 Java Virtual Machine

The heart of the Java platform is the concept of a "virtual machine" that executes Java bytecode programs. This bytecode is the same no matter what

hardware or operating system the program is running under. There is a JIT (Just In Time) compiler within the Java Virtual Machine, or JVM. The JIT compiler translates the Java bytecode into native processor instructions at run-time and caches the native code in memory during execution.

The use of bytecode as an intermediate language permits Java programs to run on any platform that has a virtual machine available. The use of a JIT compiler means that Java applications, after a short delay during loading and once they have "warmed up" by being all or mostly JIT-compiled, tend to run about as fast as native programs.[citation needed]Since JRE version 1.2, Sun's JVM implementation has included a just-in-time compiler instead of an interpreter.

Although Java programs are cross-platform or platform independent, the code of the Java Virtual Machines (JVM) that executes these programs is not. Every supported operating platform has its own JVM [36].

3.5.8 Electrical Performance Characteristics Analyzer Tool

The operation principle of the analyzer software tool is presented in this sub section with a logical flow diagram. When the software is open, first of all we have to select the com port of the computer. It should be selected automatically; if it is not selected automatically then we have to refresh the com port using the refresh port tab. Now we are ready to connect this tool with our system; so press the connect TTL tab and we will be started getting voltage current and temperature data from the solar PV module. Before we start analyze data we can clear the history from previous analysis and can clear the logs of the results. Now we have to fill the information of the module I-V characteristics given as rating in a table named summary. After completion of data input we are ready to plot the graph of the I-V and Power curve of the solar PV module. Here once we press the I-V characteristics curve and power curve (p vs v) tab then the user input table 1 will be locked and no change can made with this table. Now After plotting the curve we can view the result in the summary

tab with user input table 2. So we can compare the given data with the tested data. If we need to save this result; there is a save image tab for this option.

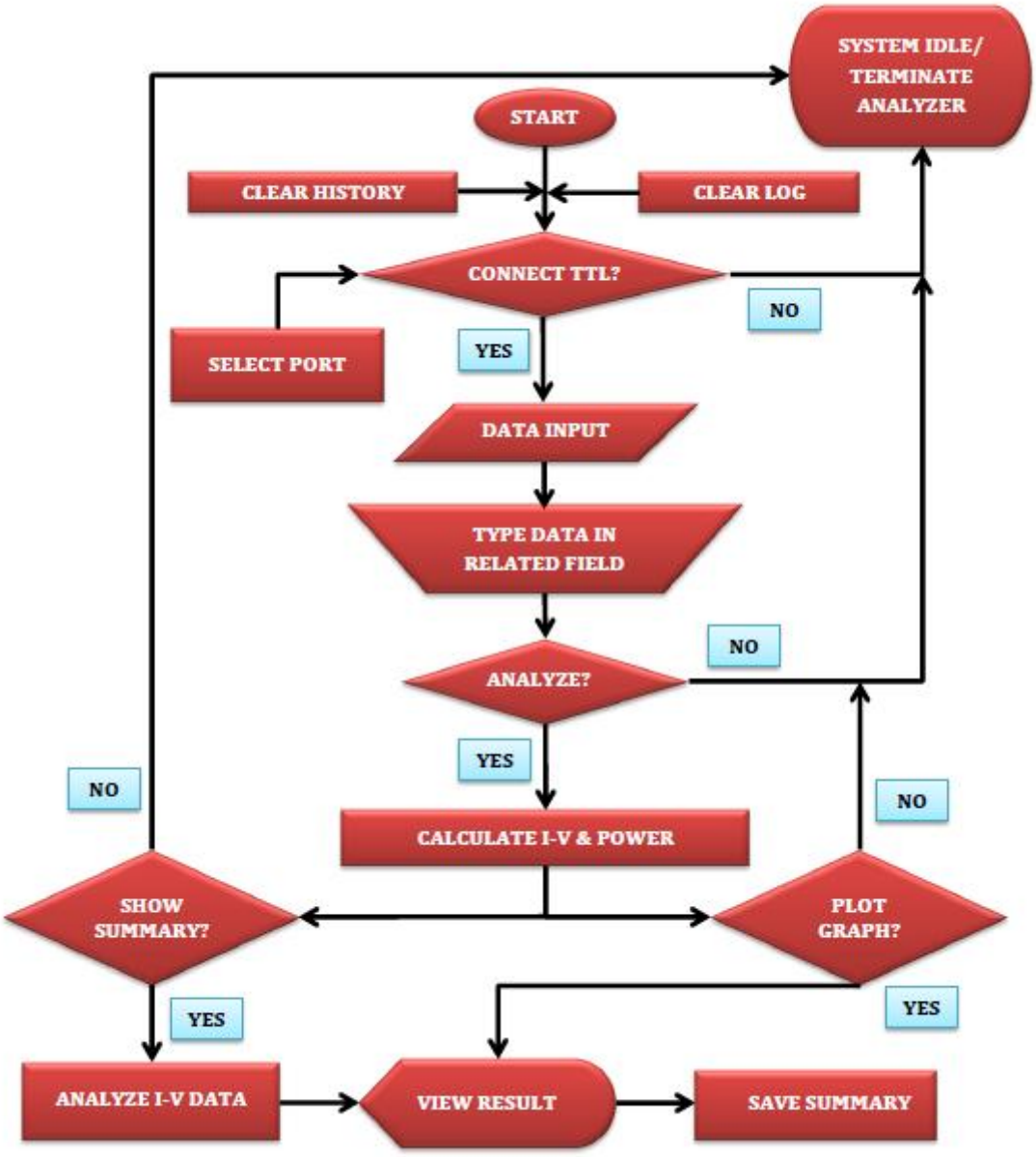

Figure 33 Flow diagram of the data analyzing software tool

Some screenshots of the software we have designed are presented below

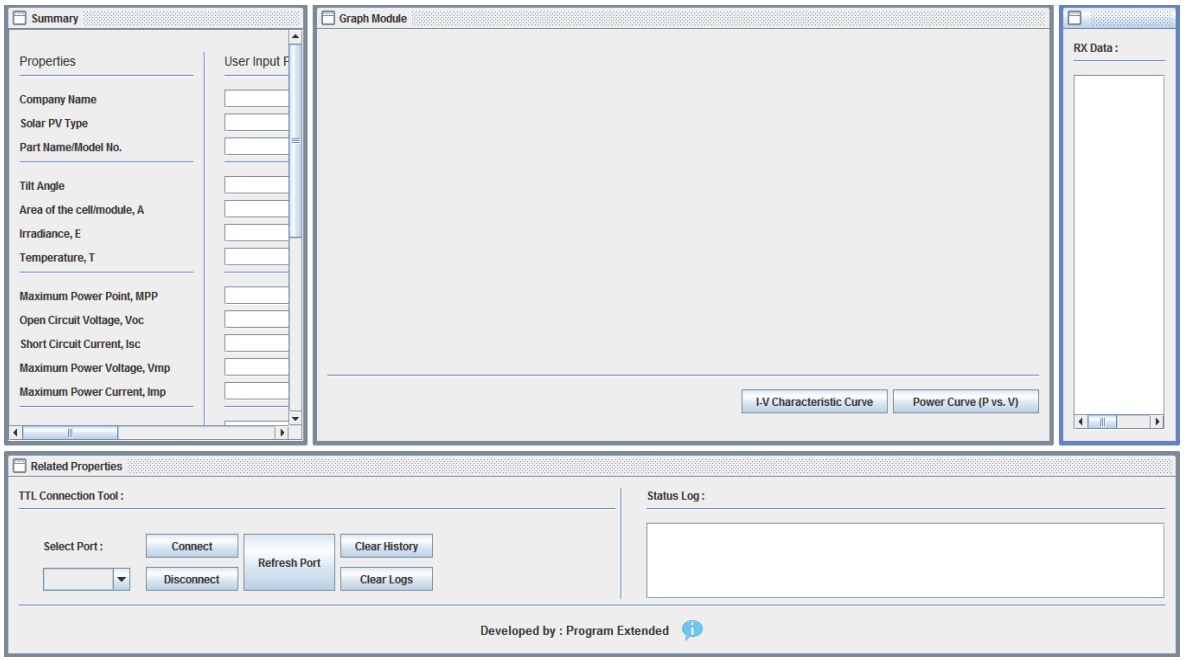

Figure 34 Graphical user interface of the analyzer software tool

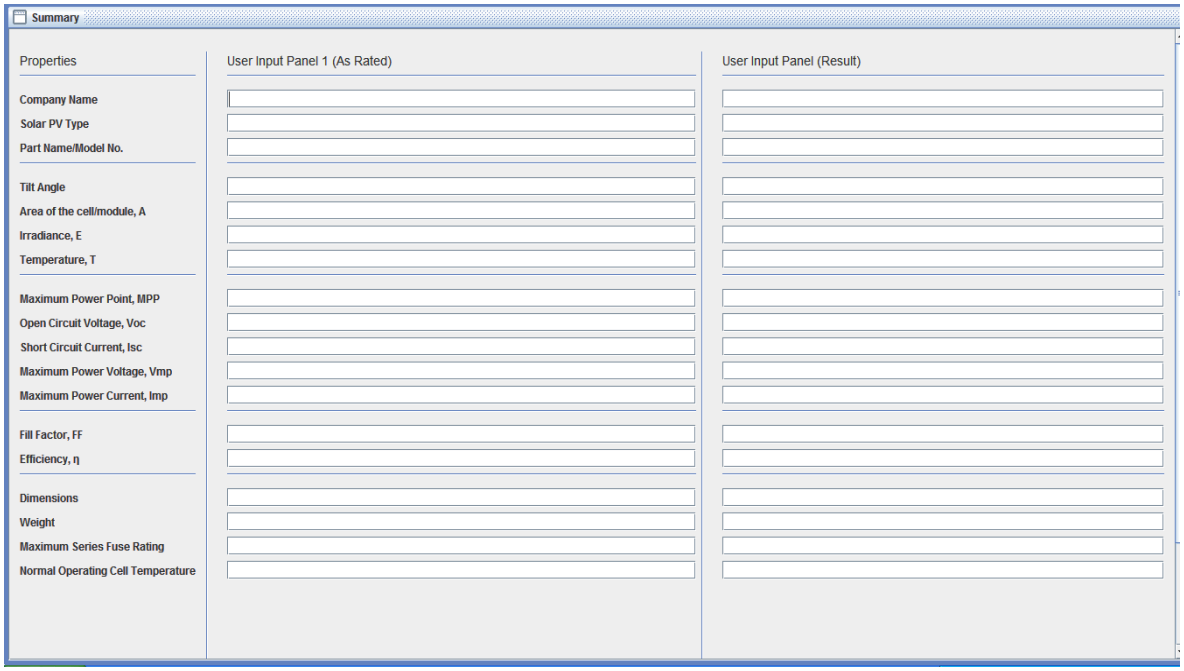

Figure 35 Summary wizard of the analyzer software tool

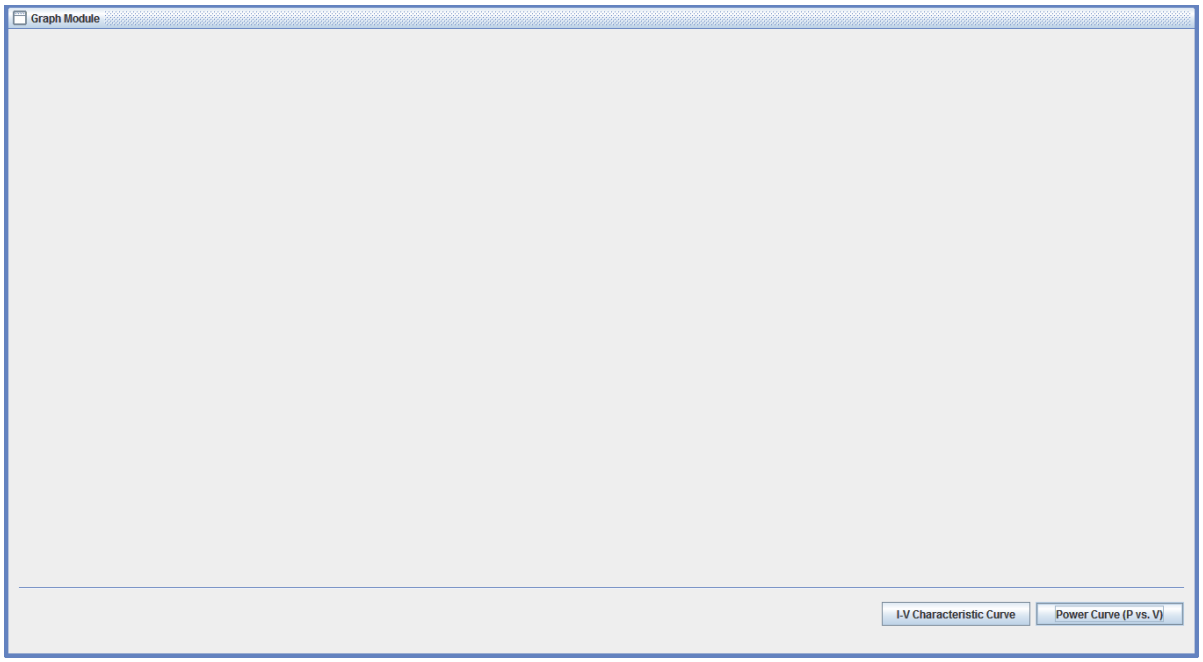

Figure 36 Graph wizard of the analyzer software tool

4 Chapter 4

Testing and Results

4.1 Result

A photo of the system we have developed is presented below

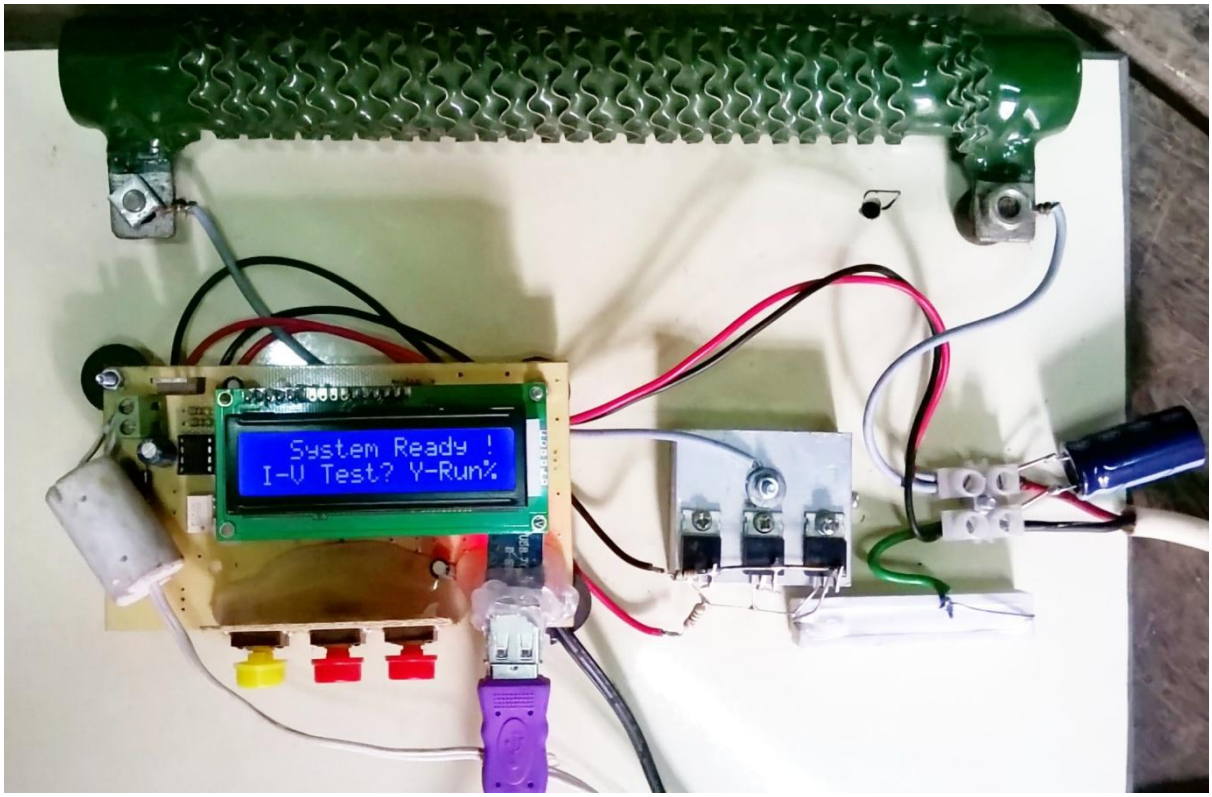

Figure 37 Practical device of the I-V Characteristic curve tracer in Operation

We have designed this system keeping in mind that all tests will be conducted in a lab with standard test condition. To ensure the standard test condition we have included temperature sensor with the system to measure the temperature of the environment and there is a field in the software tool where we can give the radiation

data collected from a pyranometer. Data from such device needs to be calculated, so we made this available in our software where when we give the pyranometer voltage data and it will calculate this data and give the result in watts.

Although we have made this system for lab condition but it will also work in actual field condition also. We have used a 50W solar PV module to test our system. The result is presented below taken from the analyzing software tool. The result generated by the PV module as the test was conducted under direct sunlight. Here PV module was on the roof of a house, and it was covered with dust. Another fact was, when we have conducted the test there was cloud cover in the sky and the weather was of end of the winter, so we have actually got very low solar radiation for our test. A photo of the PV module is presented below

Figure 38 Solar PV module (50W) that was used for testing of the system

We have tested the system for three times to get I-V data and analyze the curve. Here we present some photo of the results we have analyzed using the software tool.

First Test and Result:

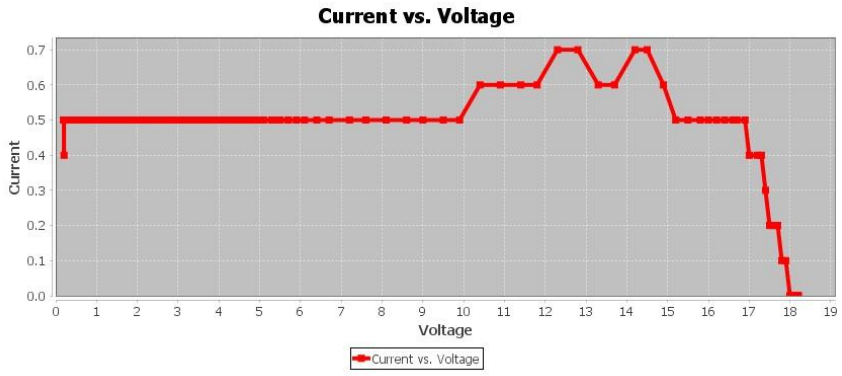

Figure 39 Current-Voltage Curve analyzed by the software in first test

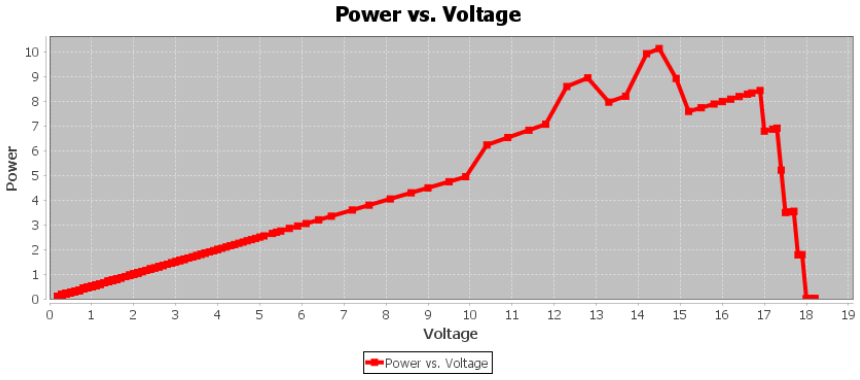

Figure 40 Power-Voltage Curve analyzed by the software in first test

Comment: In this graph we can see that the curve is not completely smooth and there exists some up-down, which is due to the availability of the sunlight we got at that moment. The current data was so small and we made the system to count only one number after the decimal. So the curve has some sharp edges. This is same for both the I-V and P-V characteristics curve.

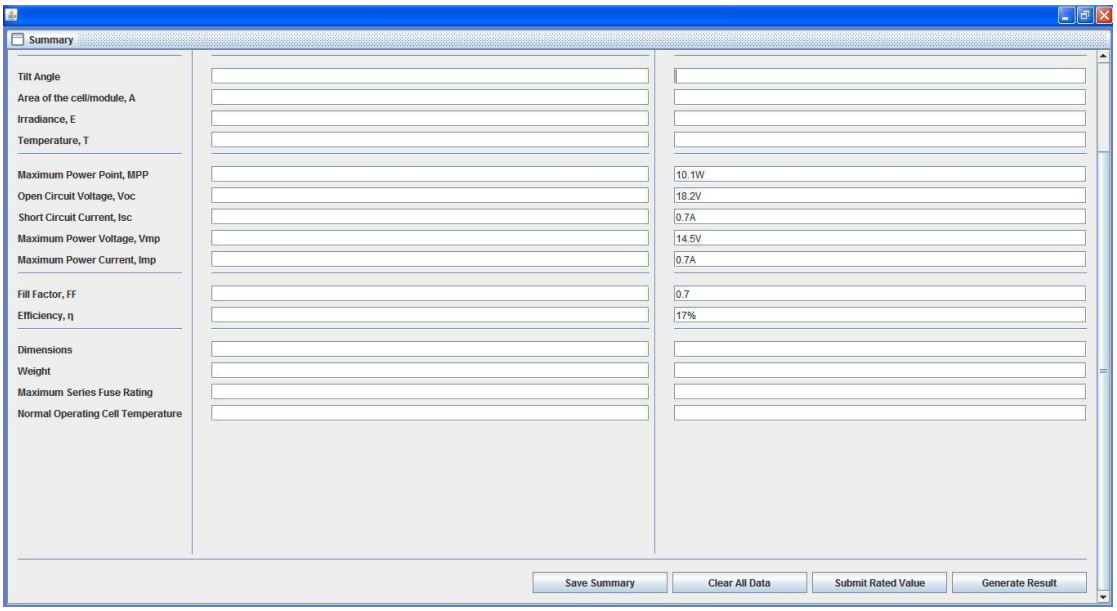

Figure 41 Result generated by analyzing the I-V characteristic curve for the first test

Second Test and Result:

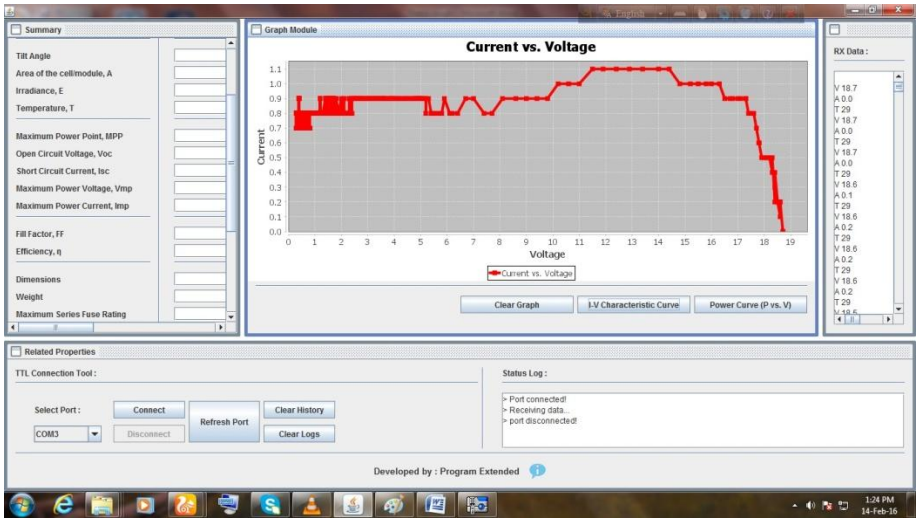

Figure 42 Current-Voltage Curve analyzed by the software in second test

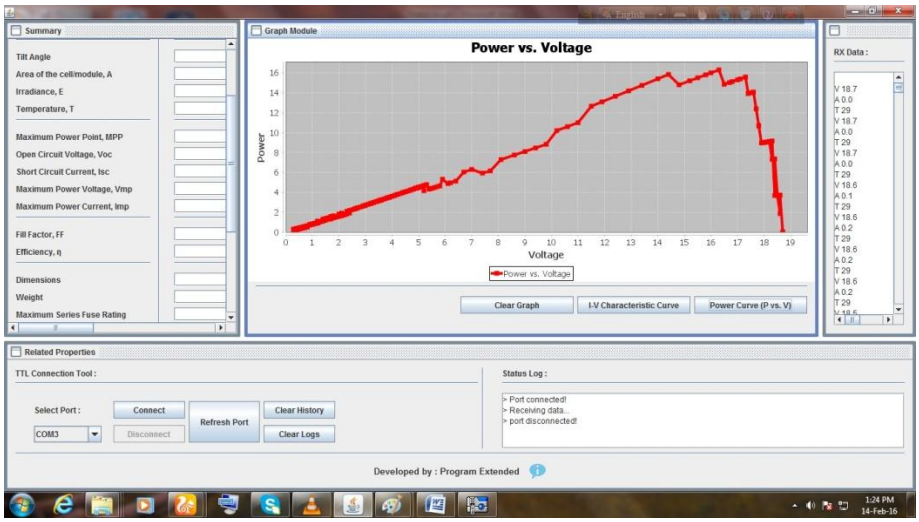

Figure 43 Power-Voltage Curve analyzed by the software in second test

Comment: In this graph we can see that the curve is not completely smooth and there exists some up-down, which is due to the availability of the sunlight we got at that moment. The current data was so small and we made the system to count only one number after the decimal. So the curve has some sharp edges. This is same for both the I-V and P-V characteristics curve.

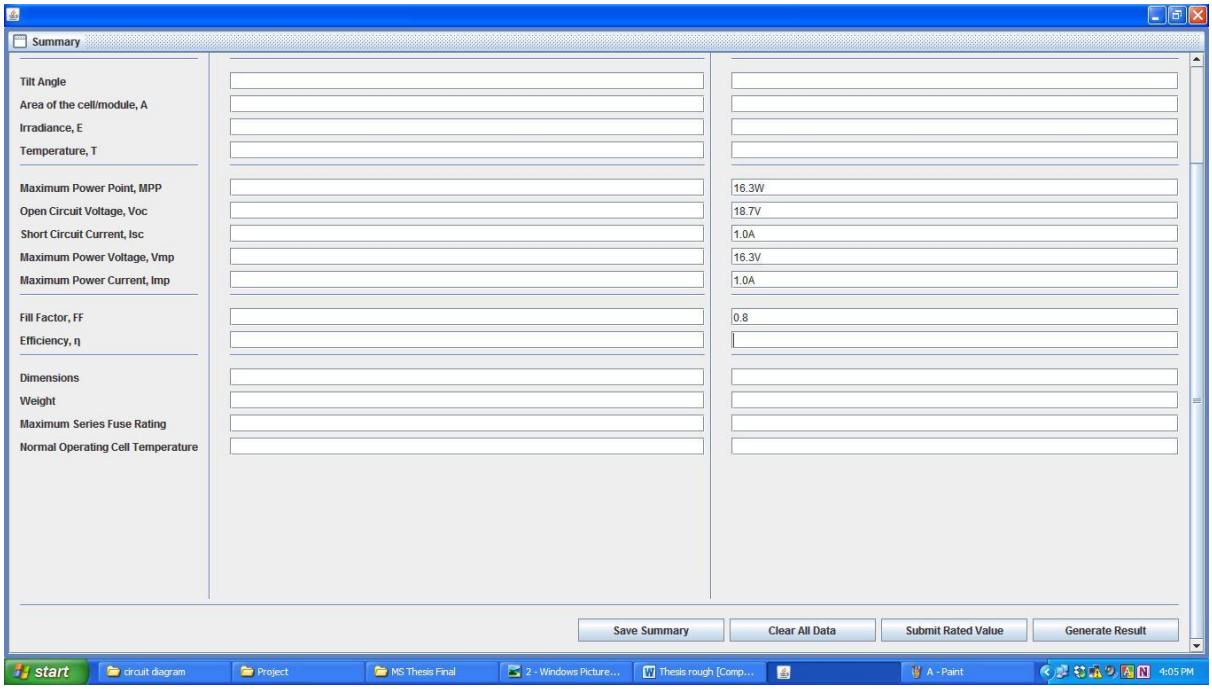

Figure 44 Result generated by analyzing the I-V characteristic curve for the second test

Third Test and Result:

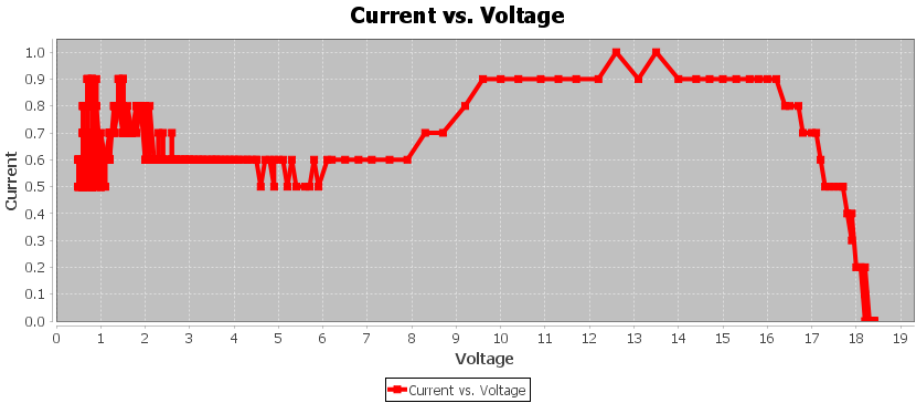

Figure 45 Current-Voltage Curve analyzed by the software in third test

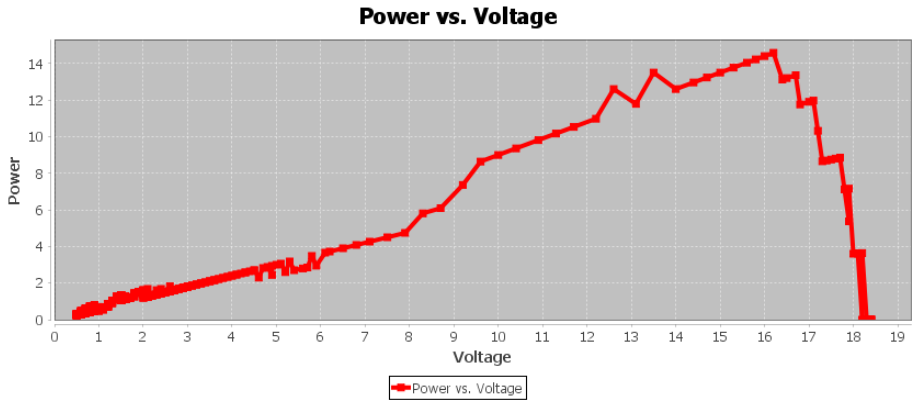

Figure 46 Power-Voltage Curve analyzed by the software in third test

Comment: In this graph we can see that the curve is not completely smooth and there exists some up-down, which is due to the availability of the sunlight we got at that moment. The current data was so small and we made the system to count only one number after the decimal. So the curve has some sharp edges. This is same for both the I-V and P-V characteristics curve.

5 Chapter 5

Conclusion and Future Work

5.1 Conclusion

As PV generation continues to grow in our country and abroad, more robust and informative monitoring equipment is necessary. I-V curves offer the most information about a PV module, but current I-V tracers require a trained technician to operate and measure the curve. So our goal was to develop a system which will reduce the effort with this I-V curve analyzing and to make the system comparably low cost one. We can say that the developed system works properly according to our first objective. Preliminary target of the system is to measure the voltage and current from the module and send the data automatically into a computer. We also wanted to build a diagnostic function for the I-V curve data and we have succeeded. So we can say through our system, quick and efficient services can be ensured such as time saving, manpower saving, cost saving manner.

Our system has some limitations too. We have used microcontroller to sense the voltage and current from the along with the MOSFET switching using PWM. We have used 10bit counter that is this system can take 1023 sets of current and voltage data along with the ambient temperature. But microcontroller operates only with binary function which is called digital system by us and we get analog output by the panel. So the problem is we cannot get complete linear data from our system. Now to sense linear data we have to modify the circuit of the system by replacing the MOSFET switching block. Our system needs +12V dc power supply to operate. We recommend using the instrument in the laboratory environment where a power supply, computer and other accessories like solar PV module and artificial lights will be available.

5.2 Future Work

Although it is a basic system to trace and analyze the electrical performance characteristics of solar PV module, but it can be improved even more up to the standard of a standalone device, in this respect the following works can be done

1. Continuous data acquisition from the solar PV module.
2. This system is capable of maximum 250W PV module measurement, so it can be extending to larger PV module than our system can measure.
3. Several solar PV modules can be measure in synchronous mode where our system only measure one module at a time.
4. The radiation data acquisition needs manual operation in our system, so this can embed with the upgrading of this system.
5. Extending the system to generate complete linear I-V data is another scope for this system.

Bibliography

1. **Laboratory, National Renewable Energy.***DOE Solar Energy Technologies Program Overview and Highlights.* Oak Ridge, TN 37831-0062 : http://www.osti.gov/scitech/, 2006. DOE/GO-102006-2314.

2. **iea.***Technology Roadmap Solar Photovoltaic Energy.* Paris, France : INTERNATIONAL ENERGY AGENCY, 2014.

3. *"Global Market Outlook for Solar Power 2015-2019" (PDF). http://www.solarpowereurope.org/. Solar Power Europe (SPE), formerly known as EPIA – European Photovoltaic Industry Association. Archived from the original on 9 June 2015. Retrieved 9 June 2015.*

4. This was the Bell Labs' first "Solar Battery." See Eric Wesoff, "Happy 60th Anniversary to the Modern Solar Cell," Greentech Media, 21 April 2014, https://www.greentechmedia.com/articles/read/Happy-60th-Anniversary-to-the-Modern-Solar-Cell. [Online]

5. *http://press.ihs.com/press-release/technology/asian-and-us-deployments-rising-ihs-raises-global-2015-solar-pv-forecast-59.*

6. Masson, op. cit. note 2; Gaëtan Masson, "40 GW in 2014 – The Sky Is Not Always the Limit," Becquerel Institute, 22 January 2015, http://becquerelinstitute.org/40-gw-2014-sky-always-limit/.

7. *Based on 2014 year-end capacity and on 70.5 GW in operation at the end of 2011, from EPIA, Global Market Outlook for Photovoltaics 2014-2018 (Brussels: 2014), p. 17, http://www.epia.org/fileadmin/user_upload/Publications/44_epia_gmo_report_ver_17_mr.pdf.*

8. **REN21.***RENEWABLES 2015 GLOBAL STATUS REPORT, Annual Reporting on Renewables:Ten years of excellence.* (Paris: REN21 Secretariat). : REN21, 2015. ISBN 978-3-9815934-6-4.

9. **Commission, General Economics Division (GED) Planning.***Final Draft SEVENTH FIVE YEAR PLAN: FY2016 – FY2020 Accelerating Growth, Empowering Citizens.* Dhaka : Planning Commission, Government of the People's Republic of Bangladesh, 13 October 2015.

10. **(IDCOL), Infrastructure Development Company Limited.***ANNUAL REPORT 2013-2014:TOWARDS A GREENER FUTURE.* Dhaka-1215, Bangladesh : Infrastructure Development Company Limited (IDCOL), 2015.

11. **Gour Chand Mazumder, Partha Ranjon Biswas, Dr. Md. Habibur Rahman.***Design and Development of an IV-Curve Plotter and Analyzer for Photovoltaic Module.* Dhaka, Bangladesh : s.n., November, 2014.

12. *NOVEL MEASURING SYSTEM FOR LONG TERM EVALUATION OF PHOTOVOLTAIC MODULES.* **Thomas Glotzbach, Jörg Kirchhof.** Kassel, Germany : Fraunhofer Institut für Windenergie und Energiesystemtechnik (IWES).

13. **www.keithley.com.** Electrical Characterization of Photovoltaic Materials and Solar Cells with the Model 4200-SCS Semiconductor Characterization System. *Drive Level Capacitance Profiling (DLCP) on PV Solar Cell Application Note Series.* CLEVELAND, U.S.A : KEITHLEY INSTRUMENTS, INC., 2011. Number 3026.

14. **Riley, Cameron William.***An Autonomous Online I-V Tracer for PV Monitoring Applications.* Tennessee, Knoxville : http://trace.tennessee.edu/utk_gradthes/3176, 2014.

15. **HabiburRahaman, Dr.** Dhaka, Bangladesh : Ph.D Thesis paper, Dept. of Applied Physics, Electronics and Communication Engineering, University of Dhaka, 2011.

16. **Authority, Energy Market.***Handbook for Solar Photovoltaic (PV) Systems.* ISBN: 978-981-08-4462-2.

17. **(ENEA), Giorgio Simbolotti.***Solar Photovoltaics Technology Brief.* s.l. : InternationalThe International Renewable Energy Agency (IRENA), Energy Agency (IEA), The Energy Technology Systems Analysis Programme (ETSAP), January 2013.

18. **THEKACKARA, M. P.***The Solar Constant and the Solar Spectrum Measured from a Reseach Aircraft.* s.l. : NASA Thchnical Report No. R-351, 1970.

19. **Green, Martin A.***SOLAR CELLS: Operating Principles, Technology, and System Applications.* s.l. : Prentice-Hall, Inc., Englewoood Cliffs, N.J. 07632. ISBN 0-13-822270-3.

20. *Annalen der Physik (4), pages 132–148, 1905.* **Einstein, A.** 6, s.l. : Annalen der Physik, 10 Mach, 2016, Vol. 322.

21. **Neamen, D.***Semiconductor Device Physics: Basic Principles,4th ed.* NY, USA, : McGraw-Hill, New York, 2012.

22. **Würfel, P.***Physics of Solar Cells (.* Weinheim, Germany : WILEY-VCH Verlag, Weinheim, 2005.

23. **Ciccone, Saverio.** vicphysics. *http://www.vicphysics.org/.* [Online] http://www.vicphysics.org/documents/events/stav2008/A7TheoryNotes.doc.

24. **TAN, YUN TIAM.***DOCTOR OF PHILOSOPHY ON IMPACT ON THE POWER SYSTEM WITH A LARGE PENETRATION OF PHOTOVOLTAIC GENERATION.* s.l. : THE UNIVERSITY OF MANCHESTER INSTITUTE OF SCIENCE AND TECHNOLOGY, FEBRUARY 2004.

25. **Christiana Honsberg, Stuart Bowden.** http://www.pveducation.org/pvcdrom/solar-cell-operation/short-circuit-current. *http://www.pveducation.org.* [Online]

26. *Contactless determination of current–voltage characteristics and minority-carrier lifetimes in semiconductors from quasi-steady-state photoconductance data.* **Sinton, RA, Cuevas, A.** s.l. : Applied Physics Letters, 1996, Vols. 69, page 2510-2512.

27. *"Electropaedia, Solar Power (Technology and Economics)".* [[Online]. Available: http://www.mpoweruk.com/solar_power.html.] : Woodbank Communications Ltd, Jan 2012 .

28. **Solmetric, The.***"Guide To Interpreting I-V Curve Measurements of PV Array,".* [http://www.solmetric.com] March, 2011.

29. **Christiana Honsberg, Stuart Bowden.** http://www.pveducation.org/pvcdrom/solar-cell-operation/fill-factor. *http://www.pveducation.org.* [Online] pveducation.org.

30. —. http://www.pveducation.org/pvcdrom/solar-cell-operation/efficiency. *PVCDROM .* [Online] pveducation.org.

31. —. http://www.pveducation.org/pvcdrom/solar-cell-operation/shunt-resistance. *PVCDROM.* [Online] pveducation.org.

32. http://www.circuitvalley.com/2012/02/30-volts-panel-volt-meter-pic.html. [Online]

33. http://www.labcenter.com/products/vsm/vsm_overview.cfm. [Online]

34. https://en.wikipedia.org/wiki/C_(programming_language). [Online]

35. http://www.codevision.be/documents.

36. http://docs.oracle.com/javase/8/docs/. [Online]

37. **Secretariat), D. S. Arora (IRADe) | Sarah Busche (NREL) | Shannon Cowlin (NREL) | Tobias Engelmeier (Bridge to India Pvt. Ltd.) | Hanna Jaritz (IRADe) | Anelia Milbrandt (NREL) | Shannon Wang (REN21).***Indian Renewable Energy Status Report: Background Report for DIREC 2010.* Oak Ridge, TN 37831-0062 : NREL/TP-6A2-48948, October 2010.

38. **Wohlgemuth, John H.***STANDARDS FOR PV MODULES AND COMPONENTS – RECENT DEVELOPMENTS AND CHALLENGES.* Golden, CO, USA : National Renewable Energy Laboratory, September 24–28, 2012.

39. *A simple resistive load I-V curve tracer for monitoring photovoltaic module characteristics. pp. 25-27.* **Willoughby, A.A.** s.l. : 5th International Renewable Energy Congress (IREC, March 2014.

40. *Field Applications for I-V Curve Tracers.* **Hernday, Paul.** Sebastopol, CA : Solmetric, Stellar Energy Solutions, 2011.

41. *http://eko-eu.com/products/photovoltaic-evaluation-systems/i-v-tracers/mp-180-i-v-tracer.* [Online]

42. *http://eko-eu.com/products/photovoltaic-evaluation-systems/i-v-tracers/mp-11-i-v-checker.* [Online]

43. s.l. : http://exploringgreentechnology.com/solar-energy/history-of-solar-energy/.

44. *https://www1.eere.energy.gov/solar/pdfs/solar_timeline.pdf.* [Online]

45. **HOWELL, R. SIEGEL AND J.R.***Thermal Radiation Heat Transfer.* Newyork : McGraw-Hill, 1972.

46. *http://www.ikonet.com/en/visualdictionary/static/us/sun.* [Online]

47. **Technology, Delft University of.** INTRODUCTION TO PHOTOVOLTAIC SOLAR ENERGY. [book auth.] Miro Zeman. *SOLAR CELLS.*

48. **(IRENA), International Renewable Energy Agency.***Solar Photovoltaics Technical Report 4.* s.l. : IRENA, 2012.

49. **(EPIA), European Photovoltaic Industry Association.***Photovoltaic Energy: Electricity from the Sun.* s.l. : EPIA, 2009.

50. —. *Global market outlook for photovoltaics 2013-2017.* s.l. : EPIA, 2013.

51. **M. A. Green. K. Emery. Y. Hishikawa. W Warta, and E. D. Dunlop.***Solar cell efficiency tables (version 41). Progress in Photovoltaics: Research and Applications, pages 1—11.* 2013.

52. *New world record efficiency for Cu(lnGa)Se2 thin-film solar cells beyond 20%. Progress in photovoltaics: Research and Applications.* **P. Jackson. D. 1-lariskos, E. Loner, S. Paetel, R. Wuerz. R. Menner. W Wischmann. And M. Powalla.** 19(7):894-897, November 2011.

53. *Solar Cell Efficiency Tables (version 37). Progress in Photovoltaics:Research and Applications.* **Green, M. A.** 19:84-92, 2011.

54. **(IEA), International Energy Agency.***PV Technology Roadmap.* s.l. : IEA, 2010.

55. **OrgaPVnet.***Technology Roadmap Towards Stable & Low Cst Oganic Bsed Slar Cells.* Brussels : s.n., 2009.

56. *Multiple exciton generation in colloidal quantum dots, singlet fission in molecules, quantum dot arrays, quantum dot solar cells, and effects of solar concentration. In Proceedings of MRS. Symposium B: Third-Generation and Emerging Solar-Cell T.* **Nozik., A.** San Francisco, California : MRS. Symposium B: Third-Generation and Emerging Solar-Cell Tecnologies, 2011.

57. *Next generation photovoltaics.* **Rafaelle, R. P.** San Francisco, California : MRS. Symposium B: Third-Generation and Emerging Sokir-Cell Technologies, 2011.

58. **(ECN), Energy Research Centre of the Netherlands.***Annual Report.* s.l. : ECN, 2012.

59. **Issolsa.***Projet BIPV - Gare TGV de Perpignan. Technical .* 2011.

60. **Gieseking, M.***BIPV. Technical.* 2011.

61. **Gonzalez, Jose Antonio Rodriguez.***Doctoral Thesis on CHARACTERIZATION, MODELLING AND OPTIMIZATION OF INDUSTRIAL THIN FILM SOLAR CELLS.* Santiago de Compostela : s.n., September 2013.

62. **Knier, Gil.** NASA Science News. *http://science.nasa.gov/.* [Online] http://science.nasa.gov/science-news/science-at-nasa/2002/solarcells/.

63. *http://www.homepower.com/articles/image/691/1936?width=750&height=600&iframe=true&template=colorbox.* [Online]

64. *Rapid and precise calculations of energy and particle flux for detailed-balance photovoltaic applications.* **Levy, MY, Honsberg, CB.** s.l. : Solid-State Electronics, 2006, Vols. 50, Page 1400-1405.

65. *On some thermodynamic aspects of photovoltaic solar energy conversion.* **Baruch, P, De Vos, A, Landsberg, PT, Parrott, JE.** s.l. : Solar Energy Materials and Solar Cells, 1995, Vols. 36, page 201-222.

66. **Christiana Honsberg, Stuart Bowden.** http://www.pveducation.org/pvcdrom/solar-cell-operation/open-circuit-voltage. [Online] pveducation.org.

67. *Solar cell fill factors: General graph and empirical expressions.* **Green, MA.** s.l. : Solid-State Electronics, 1981, Vols. 24, page 788 - 789. ISSN 00381101.

68. **Christiana Honsberg, Stuart Bowden.** http://www.pveducation.org/pvcdrom/solar-cell-operation/series-resistance. *PVCDROM.* [Online] pveducation.org.

69. *Halls, J.J. and R.H. Friend, Organic Photovoltaic devices, in Clean electricity from photovoltaics, M.D. Archer and R. Hill, Editors. 2001, Imperial College Press: London.*

Appendix A

Air mass= $(\text{Cos}\theta)^{-1}$ 2.1

$E=h\nu$ 2.2

$I_{pv} = I_p - I_D - I_{sh} = I_p - I_o \left(e^{\frac{q\,(Vpv+Rs\,Ipv)}{NKT}} - 1\right) - \frac{Vpv+Rs\,Ipv}{Rsh}$ 2.3

$J_{sc} = qG\,(L_n + L_p)$ 2.4

$$V_{OC} = \frac{nkT}{q} \ln\left(\frac{I_L}{I_0} + 1\right)$$ 2.5

$$V_{OC} = \frac{kT}{q} \ln\left[\frac{(N_A + \Delta n)\Delta n}{n_i^2}\right]$$ 2.6

$$FF = \frac{V_{MP} I_{MP}}{V_{OC} I_{SC}}$$ 2.7

$$P_{max} = V_{OC} I_{SC} FF$$ 2.8

$$\eta = \frac{V_{OC} I_{SC} FF}{P_{in}}$$ 2.9

$I=I_L - I_0 \exp[qVnkT] - VR_{SH}$ 2.10

$I=I_L - I_0 \exp[q(V+IR_S)/nkT]$ 2.11

Appendix B

```
/*****************************************************
This program was created by the
CodeWizardAVR V3.12 Advanced
Automatic Program Generator
© Copyright 1998-2014 PavelHaiduc, HP InfoTech s.r.l.
http://www.hpinfotech.com

Chip type               : ATmega32A
Program type            : Application
AVR Core Clock frequency: 8.000000 MHz
Memory model            : Small
External RAM size       : 0
Data Stack size         : 512
*****************************************************/

#include <mega32a.h>
#include <delay.h>
// I2C Bus functions
#include <i2c.h>

#define mode PINA.7
#define data_send PINA.6
#define run PINA.5
// I2C Bus functions
#include <i2c.h>
unsigned char display_buffer[20],display_buffer1[20],display_buffer2[20],display_buffer3[20];
unsigned int adc,adc1,adc2,b_adc,i_adc,aa,bb,pwm,temp;
floatb_volt,b_amps,vmax,Imax;

unsignedint set=0,s;
unsigned char b,run_button;
long  new_watt,old_watt;
unsigned char b_volt_up [1],b_volt_dn[2],new_batt_volt1,new_batt_volt2;

#define Ext_EEPROM_Adr 0xA0

unsigned char eeprom_read(unsigned char address) {
unsigned char data;
i2c_start();
i2c_write(0xa0);
i2c_write(0);
i2c_write(address);
i2c_start();
i2c_write(0xa1);
data=i2c_read(0);
delay_ms(1); //10
i2c_stop();
return data;}

unsigned char eeprom_write(unsigned char address1,char data) {
//unsigned char data;
i2c_start();
i2c_write(0xa0);
```

```
i2c_write(0);
//i2c_write(address2);
i2c_write(address1);
i2c_write(data);
i2c_stop();
return data;
delay_ms(10);//5}
// Declare your global variables here
// Alphanumeric LCD functions
#include <alcd.h>
// Declare your global variables here
#define DATA_REGISTER_EMPTY (1<<UDRE)
#define RX_COMPLETE (1<<RXC)
#define FRAMING_ERROR (1<<FE)
#define PARITY_ERROR (1<<UPE)
#define DATA_OVERRUN (1<<DOR)

// USART Transmitter buffer
#define TX_BUFFER_SIZE 8
chartx_buffer[TX_BUFFER_SIZE];

void main(void)
DDRA=(0<<DDA7) | (0<<DDA6) | (0<<DDA5) | (0<<DDA4) | (0<<DDA3) | (0<<DDA2) | (0<<DDA1) |
(0<<DDA0);
PORTA=(1<<PORTA7) | (1<<PORTA6) | (1<<PORTA5) | (0<<PORTA4) | (0<<PORTA3) |
(0<<PORTA2) | (0<<PORTA1) | (0<<PORTA0);
DDRB=(1<<DDB7) | (1<<DDB6) | (1<<DDB5) | (1<<DDB4) | (1<<DDB3) | (1<<DDB2) | (1<<DDB1) |
(1<<DDB0);
PORTB=(0<<PORTB7) | (0<<PORTB6) | (0<<PORTB5) | (0<<PORTB4) | (0<<PORTB3) |
(0<<PORTB2) | (0<<PORTB1) | (0<<PORTB0);
DDRC=(0<<DDC7) | (0<<DDC6) | (0<<DDC5) | (0<<DDC4) | (0<<DDC3) | (0<<DDC2) | (0<<DDC1) |
(0<<DDC0);
PORTC=(0<<PORTC7) | (0<<PORTC6) | (0<<PORTC5) | (0<<PORTC4) | (0<<PORTC3) | (0<<PORTC2)
| (0<<PORTC1) | (0<<PORTC0);
DDRD=(0<<DDD7) | (0<<DDD6) | (1<<DDD5) | (0<<DDD4) | (0<<DDD3) | (0<<DDD2) | (1<<DDD1) |
(0<<DDD0);
PORTD=(0<<PORTD7) | (0<<PORTD6) | (0<<PORTD5) | (0<<PORTD4) | (0<<PORTD3) |
(0<<PORTD2) | (0<<PORTD1) | (0<<PORTD0);
ADMUX=ADC_VREF_TYPE;
ADCSRA=(1<<ADEN) | (0<<ADSC) | (0<<ADATE) | (0<<ADIF) | (0<<ADIE) | (0<<ADPS2) |
(1<<ADPS1) | (1<<ADPS0);
SFIOR=(0<<ADTS2) | (0<<ADTS1) | (0<<ADTS0);
SPCR=(0<<SPIE) | (0<<SPE) | (0<<DORD) | (0<<MSTR) | (0<<CPOL) | (0<<CPHA) | (0<<SPR1) |
(0<<SPR0);
TWCR=(0<<TWEA) | (0<<TWSTA) | (0<<TWSTO) | (0<<TWEN) | (0<<TWIE);


delay_ms(10);
i2c_init();

lcd_init(16);
lcd_gotoxy(3,0);
lcd_putsf("WELCOME TO");
lcd_gotoxy(0,1);
lcd_putsf("** RET-IE-DU **");
delay_ms(2000);
lcd_clear();
```

```
// Global enable interrupts
#asm("sei")
set=1;
while (1)
{// Place your code here

    OCR1AH=bb;
    OCR1AL=aa;

if(mode==0){set=1;delay_ms(200);}
if(data_send==0){set=2;delay_ms(200);}
if(run==0){set=3;delay_ms(200);}
    X:

if(set==1){ old_watt=0;
    OCR1AH=0x00;
    OCR1AL=0x00;
lcd_gotoxy(0,0);
lcd_putsf("  System Ready !");
lcd_gotoxy(0,1);
lcd_putsf("I-V Test? Y-Run");
delay_ms(300);
if(run==0){set=4;pwm=0;run_button=1;lcd_clear();goto Y;}
if(data_send==0){set=5;pwm=0;run_button=1;goto Z;}
goto X; }

    Y:
if(set==4){ if(run_button==1 && run==1) run_button=0;
adc=0;
    adc1=0;
    adc2=0;
    OCR1AH=pwm/256;
    OCR1AL=pwm%256;
for (b=1;b<=50;b++) {
adc+=read_adc(0);  //voltage
            adc1+=read_adc(1); //current
            adc2+=read_adc(2); //temp
delay_ms(1); };
b_adc=(int)(adc/50);
i_adc=(int)(adc1/50);
temp=(int)(adc2/50);
b_volt=(float)b_adc/36.81;    //ratio
b_amps=(float)i_adc*0.078;    //ratio

new_watt=b_volt*b_amps;

if(old_watt<=new_watt){
vmax=b_volt;
Imax=b_amps;
old_watt=new_watt; }

lcd_gotoxy(0,0);
sprintf(display_buffer," %03.1fA     %3.1fV ",b_amps,b_volt);
lcd_puts(display_buffer);
delay_ms(1);
```

```
lcd_gotoxy(0,1);
sprintf(display_buffer1,"T=%02d%cC     %02d%c ",(int)temp/2,0xdf,(int)(pwm/10.23),0x25);
lcd_puts(display_buffer1);
delay_ms(1);

printf("\n\rV %2.1f",(float)b_volt);
delay_ms(5);
printf("\n\rA %2.1f",(float)b_amps);
delay_ms(5);
printf("\n\rT %02d",(int)(temp/2));
delay_ms(5);

pwm++;
if(pwm>=1024){set=1;pwm=0;goto X;}
if(run==0 &&run_button==0){set=1;goto X;}
goto Y; }

    Z:
if(set==5){ OCR1AH=0x00;
    OCR1AL=0x00;
lcd_clear();
delay_ms(100);
lcd_gotoxy(0,0);
sprintf(display_buffer1,"Vm=%03.1fV ",(float)vmax);
lcd_puts(display_buffer1);
delay_ms(10);
lcd_gotoxy(0,1);
sprintf(display_buffer1,"Im=%003.1fA ",(float)Imax);
lcd_puts(display_buffer1);
delay_ms(10);

delay_ms(2000);

set=1;goto X;}}}
```

Appendix C

Schematic diagram of the system we have developed is presented here

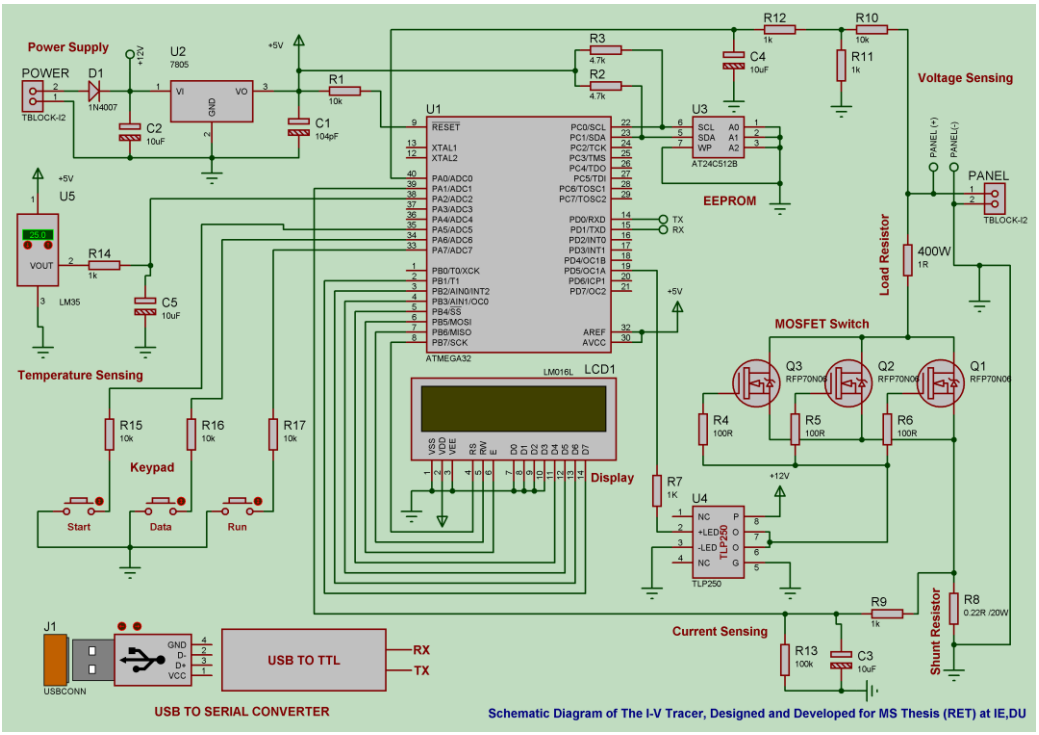

Appendix D

Printed Circuit Board of the I-V tracer